CAPITAL UNIVERSITY OF SCIENCE AND TECHNOLOGY, ISLAMABAD

Itraconazole-Loaded Polycaprolactone Nanoparticles as Versatile Nanocarriers: A Promising Strategy for Antifungal Therapy

by

Sajjad Hussain

A thesis submitted in partial fulfillment for the degree of Master of Philosophy

in the

Faculty of Pharmacy
Department of Pharmaceutics

2025

I dedicate this thesis to my loving and supportive family, friends and my supervisor, whose unwavering support has been crucial in helping me achieve my life goals.

CERTIFICATE OF APPROVAL

Itraconazole-Loaded Polycaprolactone Nanoparticles as Versatile Nanocarriers: A Promising Strategy for Antifungal Therapy

by

Sajjad Hussain

(Registration No: MPH233001)

THESIS EXAMINING COMMITTEE

S. No.	Examiner	Name	Organization
(a)	External Examiner	Dr. Syed Faisal Badshah	UoP, AJK
(b)	Internal Examiner	Dr. Mahboob Alam	CUST, Islamabad
(c)	Supervisor	Dr. Nadia Shamshad Malik	CUST, Islamabad

Dr. Nadia Shamshad Malik
Thesis Supervisor
October, 2025

Dr. Nadia Shamshad Malik
Head
Dept. of Pharmaceutics
October, 2025

Dr. Muzaffar Abbas
Dean
Faculty of Pharmacy
October, 2025

Author's Declaration

I, **Sajjad Hussain** hereby state that my M.Phil thesis titled "**Itraconazole-Loaded Polycaprolactone Nanoparticles as Versatile Nanocarriers: A Promising Strategy for Antifungal Therapy**" is my own work and has not been submitted previously by me for taking any degree from Capital University of Science and Technology, Islamabad or anywhere else in the country/abroad.

At any time if my statement is found to be incorrect even after my graduation, the University has the right to withdraw my M.Phil Degree.

(Sajjad Hussain)

Registration No: MPH233001

Plagiarism Undertaking

I solemnly declare that research work presented in this thesis titled "**Itraconazole-Loaded Polycaprolactone Nanoparticles as Versatile Nanocarriers: A Promising Strategy for Antifungal Therapy**" is solely my research work with no significant contribution from any other person. Small contribution/help wherever taken has been duly acknowledged and that complete thesis has been written by me.

I understand the zero tolerance policy of the HEC and Capital University of Science and Technology towards plagiarism. Therefore, I as an author of the above titled thesis declare that no portion of my thesis has been plagiarized and any material used as reference is properly referred/cited.

I undertake that if I am found guilty of any formal plagiarism in the above titled thesis even after award of M.Phil Degree, the University reserves the right to withdraw/revoke my M.Phil degree and that HEC and the University have the right to publish my name on the HEC/University website on which names of students are placed who submitted plagiarized work.

(Sajjad Hussain)

Registration No: MPH233001

Acknowledgement

I am grateful to Allah Almighty for the countless blessings He has bestowed upon me. I am deeply thankful for everything I have received and will receive in my life. I appreciate the numerous miracles that have occurred for my benefit.

I would like to express my extreme gratitude to my supervisor, **Dr. Nadia Shamshad Malik** for her wonderful help and dedication. This thesis was planned, and the writing was done, with her help. I am also very grateful to **Dean Dr. Muzaffar Abbas**. Their encouragement, guidance and support in my academic journey has been a huge role for me and their mentorship has been a big source of inspiration.

I am forever grateful to my family and my friends for their weekly unwavering support, and their never ending guidance. Love, wisdom and sacrifices of theirs had made me what I am now. I owe to their unceasing faith in me and their heartfelt involvement, which inspires me.

(Sajjad Hussain)

Abstract

Itraconazole (ITZ) is a BCS class II antifungal agent. It is a difficult to formulate due to its poor water solubility (<0.2 mmol /mL) and variable oral bioavailability (∼55 %). The aim of this study was to develop Polycaprolactone (PCL) nanoparticles to improve its transdermal delivery. The nanoparticles were prepared using a modified nanoprecipitation method, resulting in ten formulations (F1 to F10). Among these, F2 (containing 40 mg PCL and 2% Poloxamer 407), showed the best properties: particle size of 154.6 nm, polydispersity index (0.378), zeta potential (-10.7 ± 5.36 mV), and encapsulation efficiency (85.4 ± 1.2%). In-vitro release studies showed a pH-dependent sustained release profile, with a cumulative drug release of 80.41% at pH 5.5 and 94.34% at pH 7.4 over 24 hours. The release followed the Higuchi kinetics ($R^2 = 0.9804$ at pH 5.5), showing a diffusion-controlled behaviour. The pH response was supported by swelling studies, which showed a swelling ratio of 1.415-1.385. Optimized nanoparticles were incorporated in a carbopol-based nanogel and showed suitable topical properties (Q_{24}: 173.29 ± 3.12 μg/cm^2); J_{ss}: 7.22 ± 0.15 μg/cm^2/h compared to a plain ITZ gel (Q_{24}: 75.35 ± 1.35 μg/cm^2; J_{ss}: 3.11 ± 0.08 μg/cm^2/h). Ex vivo penetration studies on F2 in rabbit skin revealed a significantly increased penetration (Q_{24}: 75.35 ± 0.12 μg/cm^2; J_{ss}: 7.11 ± 0.08 μg/cm^2/h) nanogel, with an enhancement ratio (ER) of 2.32. The improved permeability can be attributed to the smaller size of the particles, and surfactant-mediated skin penetration. The DSC, XRD and FTIR characterizations confirmed the amorphous nature of ITZ and the absence of drug-drug interactions. Skin irritation testing (Draize test) showed excellent dermal safety (PII= 0) with no signs of erythema or swelling. Stability studies for Three-month according to ICH Q1A(R2) showed minimal variations in pH (±0.5) and viscosity (<8%). These observations highlight the development of nanogel based on PCL as a promising and biocompatible ITZ transdermal system offering pH-responsive sustained release, increased skin permeability and increased therapeutic efficacy in antifungal therapy.

Contents

List of Figures

List of Tables

Abbreviations

ANOVA	Analysis of Variance
DSC	Differential Scanning Calorimetry
EE	Encapsulation Efficiency
FTIR	Fourier-Transform Infrared Spectroscopy
ITZ	Itraconazole
MWCO	Molecular Weight Cut-Off
NLCs	Nanostructured Lipid Carriers
PCL	Polycaprolactone
PDI	Polydispersity Index
EDDS	Self-Emulsifying Drug Delivery Systems
SEM	Scanning Electron Microscopy
SLNs	Solid Lipid Nanoparticles
TDDS	Transdermal Drug Delivery System
TGA	Thermogravimetric Analysis
XRD	X-ray Diffraction

Chapter 1

Introduction

1.1 Epidemiology and Clinical Burden of Fungal Infections

Fungal infections represent a growing global health challenge, especially in immunocompromised patients and those suffering from chronic disease; the incidence and severity of invasive fungal infections have increased over the past two decades due to medical interventions such as organ transplants, chemotherapy, and immunosuppressive therapy that can compromise immune function. It has been estimated that more than one billion people suffer from some form of fungal disease every year and that invasive fungal infections cause greater than 1.5 million deaths per year, making their mortality rates comparable with those for tuberculosis and malaria [1].

Superficial infections such as dermatophytosis, onychomycosis, and candidiasis are among the most common forms of superficial mycoses; they affect about 20% to 25% of the world population, occur frequently in both developed and developing countries. These infections cause physical discomfort, constitute a substantial economic burden on healthcare systems because they tend to be chronic and recurrent, and are not life-threatening but do severely impact quality of life and can also serve as portals for more serious secondary infections in immunocompromised

hosts [2]. With higher rates of antifungal resistance emerging, especially in Candida and Aspergillus species, the overexpression of efflux pumps, target enzyme mutations, and biofilm formation have rendered standard antifungals ineffective; this is particularly alarming given that C. auris is a multidrug-resistant fungal pathogen causing hospital outbreaks worldwide with high mortality [3][4].

The use of antifungal peptides is a new approach to solving this problem. These peptides are relatively small proteinaceous molecules that can be designed specifically for targeting fungi and their unique cell wall components. They also have advantages over conventional drugs in terms of specificity, low toxicity, and rapid action [5].

Antibiotics are chemical compounds used to treat diseases caused by infectious agents. Traditional antifungals like polyenes, azoles, and echinocandins have many limitations: toxicity, drug–drug interactions, narrow therapeutic index, and poor tissue penetration. Prolonged therapy is often required for clinical management of fungal infections, which raises the risk of resistance and adverse effects.

Furthermore, poor drug distribution to infected tissues, particularly in cases of deep-seated or disseminated infections, is frequently preventing effective systemic antifungal therapy. These pharmacological challenges require the development of novel delivery systems that can enhance therapeutic efficacy while minimizing systemic toxicity [6]. Adding to the clinical burden, the diagnosis of fungal infections remains a major challenge. Usually, conventional diagnostic tools lack sensitivity and specificity, which leads to delayed treatment initiation.

This delay can have dire consequences, particularly in invasive infections like fungal keratitis or fungal meningitis, where early intervention is critical for survival. Accurate, rapid, and cost-effective diagnostic tools will go hand-in-hand with more targeted and effective antifungal delivery systems as we develop new ways to treat fungal infections in a more directed fashion. As the prevalence of fungal infection increases, along with emerging resistance and suboptimal current antifungal therapy, the need for novel drug delivery platforms that can maximize bioavailability, tissue targeting, and therapeutic index is becoming increasingly important.

1.2 Itraconazole as a Broad-Spectrum Antifungal: Therapeutic Potential and Delivery Challenges

The cytochrome P450 enzyme lanosterol 14-demethylase, which is involved in ergosterol biosynthesis and supports fungal cell viability and membrane integrity, is inhibited by Itraconazole (ITZ), a second-generation triazole antifungal. ITZ exhibits fungicidal or broad-spectrum fungistatic activity against Candida species. Aspergillus species. Blastomyces dermatitidis, Histoplasma capsulatum, and dermatophytes [7]. The clinical utility of the drug is limited by its physicochemical properties; Itraconazole is extremely insoluble in water (solubility < 1 μg/mL) and has been designated a Biopharmaceutics Classification System (BCS) Class II compound (poorly soluble but highly permeable) [8]. Moreover, it has pH-dependent solubility; absorption is optimal in an acidic gastric environment, and its bioavailability is reduced significantly by elevation of gastric pH caused by proton-pump inhibitors or antacids (typically 30% to 55%). ITZ also undergoes extensive hepatic metabolism via cytochrome P450 (CYP3A4), has high plasma protein binding ($\sim$99%), and demonstrates considerable pharmacokinetic complexity and high inter individual variability, all of which makes therapeutic drug monitoring (TDM) crucial for optimal serum levels, particularly in immunocompromised patients. Topical formulations also are challenging due to low percutaneous permeability, poor retention at the site of infection, and rapid systemic clearance; therefore, enhanced solubility, stability, and local retention remain a focus in the development of antifungal therapy [9].

1.3 Addressing Biopharmaceutical Limitations through Nanotechnology

Nanotechnology offers a promising platform to enhance the solubility, permeability, and efficiency of poorly water-soluble drugs, including ITZ, by reducing the particle

size down to the nanometer scale, which increases surface area for dissolution rates; controlled drug release and site-specific targeting reduces systemic side effects and enhances local therapeutic action [10].

They can penetrate biological barriers such as the stratum corneum to deliver medication more deeply into the skin or other tissues, leading to lower dosages and less side effects in antifungal therapy. These nanoparticles have shown enhanced therapeutic efficacy and drug bioavailability in animal models [11].

Nanotechnology enables drug delivery through transdermal applications, removing the need for first-pass hepatic metabolism and systemic administration. In addition to offering the potential for controlled and pH-responsive release in infected tissues, nanoparticles can be engineered with penetration enhancers and surfactants to facilitate skin penetration [12].

1.4 Polycaprolactone Nanoparticles for Drug Delivery: Biocompatibility and Release Modulation

In this respect, polycaprolactone (PCL) has been reported as a semicrystalline, biodegradable, and biocompatible polyester with FDA approval for various biomedical applications such as sutures, implants, and drug delivery systems, which has shown to have high encapsulation efficiency and controlled release profiles that can be tuned by polymer concentration, molecular weight, and formulation method [13].

It is also hydrophobic and suitable for poorly water-soluble drugs like ITZ, it degrades slowly, and the polymer is stable under physiological conditions and does not produce toxic degradation products; thus, PCL nanoparticles may be appropriate for chronic use. Several studies have demonstrated the use of PCL in encapsulating antifungal agents, resulting in improved skin penetration, reduced

dosing frequency, and improved clinical outcomes. Further development of multifunctional delivery platforms for targeted antifungal therapy is possible because PCL is compatible with a wide range of surfactants, plasticizers and co-polymers [14].

1.5 Rational Formulation Design: Synergistic Role of PCL, Poloxamer 407, and Carbopol 934 in Nanogel Systems

A rational approach to ITZ formulation involves selecting excipients that act synergistically to stabilize the nanoparticles, improve skin permeation, and provide a suitable vehicle for topical delivery. PCL is used as the core polymer to encase ITZ and modify its release profile in this study. It is used as a surfactant and stabilizer. It also enhances skin permeability by disrupting the lipid matrix of the stratum corneum [15].

The nanoparticle suspension is converted into a nanogel using Carbopol 934, which acts as a gelling agent to provide rheological stability and enhance drug retention at the application site while ensuring bioadhesion to the skin. The combination of nanoparticles (improved delivery and controlled release) and gels (ease of administration and prolonged contact time) results in an ideal platform for transdermal delivery of ITZ [16].

1.6 Research Aims and Objectives

The main aim of this study is to explore a new polycaprolactone (PCL)-based nanogel system for the transdermal delivery of Itraconazole (ITZ) to overcome biopharmaceutical limitations such as poor aqueous solubility, low bioavailability, and systemic toxicity with conventional ITZ formulations. By using a nanotechnology-based strategy, this research aims to enhance skin permeation, enable controlled

drug release, and improve localized antifungal efficacy, while minimizing systemic side effects. The Objectives of the study are:

1.6.1 Formulation Development of ITZ-Loaded PCL Nanoparticles

To utilize a modified nanoprecipitation technique for creating and optimizing various formulations of polycaprolactone (PCL) nanoparticles loaded with Itraconazole (ITZ), with variations in:

- Polymer-to-drug ratio (PCL:ITZ)
- Surfactant concentration (Poloxamer 407)
- Aqueous-to-organic phase ratio
- Entrapment efficiency (EE)
- Stability under simulated physiological conditions (pH, temperature, ionic strength)

1.6.2 Nanogel Development

To develop an optimized ITZ–PCL nanoparticle delivery system within a Carbopol 934 gel matrix and evaluate:

- Bioadhesion and rheological properties
- Sustained release profile
- Influence of functional excipients (Poloxamer 407 and eucalyptus oil) on:
- Viscosity
- Spreadability

- pH compatibility (target skin pH: 5.5–6.0)
- Drug release kinetics (diffusion vs. erosion mechanisms)
- Ex vivo skin permeation performance

1.6.3 Characterization of Physicochemical and Functional Properties To characterize the developed formulations using:

- Dynamic Light Scattering (DLS): Particle size and polydispersity index (PDI)
- Zeta Potential: Assessment of colloidal stability
- Scanning Electron Microscopy (SEM): Surface morphology
- Differential Scanning Calorimetry (DSC) & Thermogravimetric Analysis (TGA): Thermal behaviour
- X-ray Diffraction (XRD) & Fourier-Transform Infrared Spectroscopy (FTIR): Crystallinity and molecular interactions

1.6.4 In Vitro and Ex Vivo Performance Evaluation

To evaluate the drug release and skin permeation characteristics:

- Perform in vitro drug release studies at pH 5.5 and 7.4 to investigate pH-responsive behaviour
- Model release kinetics using zero-order, first-order, Higuchi, and Korsmeyer-Peppas models
- Conduct ex vivo permeation studies on excised rabbit skin to quantify:
- Cumulative drug permeation over 24 hours (Q_{24})

- Steady-state flux (Jss)
- Enhancement ratio (ER) compared to conventional ITZ gels

1.6.5 Biocompatibility and Stability Assessment

- Assess skin safety using the Draize skin irritation test in New Zealand white rabbits by evaluating erythema, edema scores, and calculating the Primary Irritation Index (PII) with a target PII 0.5
- Conduct accelerated stability testing under ICH guidelines for 3 months at 4°C, 25°C,40°C with 75% relative humidity

Chapter 2

Literature Review

2.1 Pharmacological Promise vs. Formulation Barriers of Itraconazole

Itraconazole (ITZ) is a triazole antifungal with broad-spectrum clinical activity that inhibits the fungal cytochrome P450 enzyme lanosterol 14-α-demethylase involved in ergosterol biosynthesis, which is necessary for cell membrane integrity. ITZ has significant activity against dermatophytes, Candida species, Aspergillus, Histoplasma and other deep-seated mycoses and is used topically as well as systemically [17].

Despite its robust pharmacological profile, the clinical application of Itraconazole is significantly restricted by several physicochemical and biopharmaceutical challenges. One of the most critical limitations is its poor aqueous solubility, which is approximately 1 ng/mL at neutral pH.

This extreme hydrophobicity poses a significant barrier to formulation scientists attempting to achieve effective and consistent drug delivery. Furthermore, its dissolution rate is pH-dependent, with optimal solubility occurring only in acidic environments ($pH < 2$), thereby limiting its absorption under normal and variable gastrointestinal conditions [18].

The variable solubility translates into inconsistent oral bioavailability in clinical settings; absorption is dependent on many factors, such as co-administration with food and acidic beverages, gastric pH, and gastrointestinal motility. This can lead to subtherapeutic plasma concentrations of Itraconazole, resulting in treatment failure or resistance. Moreover, Itraconazole undergoes extensive first-pass metabolism in the liver via the cytochrome (CYP3A4) enzyme system. This metabolism leads to the formation of several metabolites, the most notable of which is hydroxy-itraconazole, which has antifungal activity. Nevertheless, hepatic metabolism significantly reduces the bioavailability of the parent compound, complicating dose optimization and increasing the likelihood of drug–drug interactions. This interaction profile requires careful monitoring and dosage adjustments in patients receiving multiple therapy, thus limiting itraconazole's broader clinical utility [19].

Additional shortcomings are also present in the conventional oral forms of ITZ, including capsules and oral suspensions. Capsules containing the drug in pelletized form show delayed dissolution unless they are taken with a full meal and an acidic beverage. Oral suspensions are less patient-friendly due to their unpleasant taste and the need for frequent dosing. On the other hand, topical formulations such as creams and ointments face challenges in skin penetration and retention. Their inability to breach the stratum corneum efficiently results in limited drug deposition at the target site, particularly in deep-seated dermal infections [20].

Another significant challenge is the poor membrane permeability of ITZ because it has a large molecular weight and lipophilic nature, which inhibits its passive diffusion across the intestinal mucosa or through skin; this means that non-invasive delivery systems are not very effective. As such, there exists an opportunity for new formulation strategies to increase solubility, control release, and improve penetration across biological membranes [21]. Given these challenges, researchers have begun to explore more advanced drug delivery systems designed to overcome these formulation barriers; however, none has yet fully resolved the complex limitations of ITZ delivery, so there is a need for a multifunctional delivery platform that would ensure consistent levels of the drug in the bloodstream and improved

bioavailability as well as compliance. In view of these difficulties, researchers have investigated advanced drug delivery systems to overcome these formulation barriers; various strategies, such as complexation with cyclodextrins, preparation of solid dispersions, or encapsulation in lipid-based or polymeric nanoparticles, have been explored but have not entirely resolved the multifaceted limitations on ITZ delivery. Hence, a multifunctional delivery platform that ensures constant drug levels in the bloodstream, improved bioavailability and patient compliance is required. In view of these difficulties, researchers have investigated advanced drug delivery systems to overcome these formulation barriers; various strategies, such as complexation with cyclodextrins [22], Nanotechnology-based delivery systems may overcome some of these challenges by reducing particle size to the nanometer range increases surface area and improves dissolution rates for ITZ while also protecting it from degradation by encapsulating it in biodegradable carriers such as polycaprolactone nanoparticles that remain on the skin longer when mixed with bioadhesive and thermoresponsive gels [23].

Although Itraconazole is a mainstay in antifungal pharmacotherapy owing to its broad-spectrum activity and clinical efficacy, the full potential of this drug has been limited by several physicochemical and biological barriers that need to be overcome through formulation strategies for increased solubility, stability, bioavailability, and reduced systemic side effects.

The subsequent sections of this chapter describe how such approaches, especially those based on polymeric nanocarriers and transdermal nanogels, are being used to realize the clinical potential of Itraconazole.

2.2 Limitations of Conventional Delivery Systems: A Biopharmaceutical Insight

Despite the availability of Itraconazole in multiple conventional formulations, such as capsules, oral suspensions, and topical creams, the efficacy of these systems

remains limited due to significant biopharmaceutical shortcomings. These drawbacks affect drug solubility, gastrointestinal (GI) metabolism, patient adherence, and the ability to deliver therapeutically adequate concentrations to target sites [24].

Its dissolution behaviour is dependent on the pH and must be taken with food to improve absorption. However, the presence of food only partially compensates for the effects of gastric pH variability. Patients on proton pump inhibitors or those with achlorhydria experience greatly reduced absorption, contributing to therapeutic inconsistency. Although oral suspensions are more bioavailable, they have drawbacks, such as a bad taste, the need to be taken at specific times with meals, and the possibility of microbial contamination, particularly in warm climates. Due to these drawbacks, oral Itraconazole treatment has become less appealing for some patient groups, such as the elderly or those who need to take several drugs that alter stomach pH [25].

In addition, while topical formulations are commonly applied for superficial infections, they are not very effective therapeutically due to the poor permeability of drugs through the skin as well as ITZ's hydrophobic nature; patients need prolonged application times, increasing the risk of non-compliance and recurrence [26]. These systems are suboptimal for sustained therapy because of transient retention on the skin surface along with an inability to control drug release. In addition, traditional topical systems often require multiple daily applications that can result in poor adherence and inadequate clinical outcomes.

Itraconazole has low oral bioavailability due to extensive hepatic metabolism by CYP3A4 enzymes and many clinically significant drug-drug interactions occur through this pathway (especially when drugs that act as inducers or inhibitors of CYP3A4 are co-administered), making treatment plans more challenging, particularly in polypharmacy settings such as immunocompromised patients, Itraconazole is a CYP3A4 inhibitor and can increase the plasma concentrations of concurrently administered medications that require therapeutic monitoring [27]. Another key issue is the variation of absorption due to GI motility and physiological status;

for example, gastric emptying time, intestinal pH, and mucosal integrity can all significantly change Itraconazole absorption, resulting in high interpatient variability, particularly among patients with compromised gut function (e.g., chemotherapy, inflammatory bowel disease, ostgastrointestinal surgery), making therapeutic concentrations unpredictable and compromising clinical efficacy while promoting resistance [28].

Furthermore, oral and topical forms are also limited clinically by inter-patient variability (due to factors such as patient-specific conditions, age, motility disorders, etc.) that complicate standardization of dosage. Other barriers to compliance include the frequent dosing and dietary restrictions required with conventional systems, especially in pediatric and geriatric populations. Itraconazole hinders systemic distribution after absorption due to extensive binding to plasma proteins and sequestration into adipose tissue, which can alter pharmacokinetics in obese individuals [29]. Together these factors demonstrate the limitations of conventional Itraconazole formulations for achieving long-term antifungal therapy, and their shortcomings in oral and topical delivery (e.g., low aqueous solubility, pH-dependent absorption, hepatic metabolism, permeability barriers) necessitate new delivery platforms that increase absorption, reduce side effects, and improve patient adherence, prompting the development of alternative approaches to drug delivery [30]. Other emerging technologies that are being increasingly explored to circumvent these limitations include solid lipid nanoparticles, polymeric micelles, and nanocarr-ier-based delivery. These systems aim at improving ITZ permeability, sustained release, solubility, and reducing the variability of drug absorption, thereby improving its pharmacokinetic and pharmacodynamic profiles [31].

2.3 Nanotechnology Interventions for Hydrophobic Antifungal Agents

Nanotechnology represents a new approach to overcoming the intrinsic limitations of poorly soluble drugs like Itraconazole (ITZ) by encapsulating hydrophobic drugs

into nanocarriers that confer several biopharmaceutical advantages, including increased aqueous solubility, protection from enzymatic degradation, enhanced permeation, and controlled release; these are essential features for antifungal agents with narrow therapeutic windows requiring precise dosing and prolonged tissue exposure to achieve eradication of deep-seated infections.

It has also been demonstrated that lipid-based systems, such as solid lipid nanoparticles (SLNs), nanostructured lipid carriers (NLCs) and self-emulsifying drug delivery systems (SEDDS), can improve the solubility and bioavailability of ITZ due to their hydrophobic entrapment in a stable environment with biocompatibility and reduced hepatic first-pass metabolism as well as prolonged systemic circulation [32].

These nanoparticles have also shown promising results in antifungal delivery. These materials have been utilized to develop nanoparticles capable of improving drug retention and bioavailability. According to [33], PLGA-based nanoparticles loaded with ITZ demonstrated improved antifungal efficacy and prolonged drug release. Further modifying surface charge and particle size allows for fine-tuning of drug delivery profiles and tissue targeting.

Another approach under investigation involves the use of nanocrystal formulations in which the particle size is reduced to the nanometer scale without a carrier matrix for increasing surface area and improving dissolution rate; compared with traditional formulations, ITZ nanocrystals showed significantly higher rates of dissolution that improved systemic exposure and therapeutic efficacy [34]. Moreover, hybrid systems combining lipids and polymers have also been investigated to maximize the advantages of both platforms. For example, lipid–polymer hybrid nanoparticle formulations of ITZ have provided superior skin permeation and antifungal activity in comparison to conventional creams, suggesting their potential for the treatment of cutaneous mycoses [35].

The nanocarriers can also deliver the product to the target site. Targeted delivery reduces off-target effects and minimizes systemic toxicity, which is critical

for antifungal therapy where prolonged systemic exposure may lead to hepatotoxicity or QT prolongation. They have demonstrated enhanced delivery of ITZ to infected tissues and intracellular fungal reservoirs. Nanotechnology not only addresses the solubility and stability challenges of Itraconazole but also opens the way for innovative, targeted, and patient-compliant antifungal therapy. These systems collectively overcome the pharmacokinetic hurdles that hinder conventional formulations and establish a platform for consistent and potent antifungal therapy [36].

2.4 Biodegradable Nanoparticles: Comparative Analysis of PCL, PLGA, and Chitosan-Based Systems

The development of biodegradable polymeric nanoparticles has revolutionized the field of drug delivery by enhancing therapeutic efficacy while lowering systemic toxicity, which can be achieved through their controlled release profiles. Various biodegradable polymers have been explored; however, among them polycaprolactone (PCL), poly (lactic-co-glycolic acid) (PLGA), and chitosan are commonly used for the encapsulation of insoluble drugs such as Itraconazole (ITZ). PCL is an FDA-approved semi-crystalline hydrophobic polyester with a slow degradation rate, high permeability to small molecules, good mechanical strength, and biocompatibility. Thus, PCL is a useful matrix for developing sustained-release formulations [37].

The high encapsulation efficiencies and sustained antifungal activity over several days observed with PCL nanoparticles have been reported for antifungal applications and their hydrophobic nature provides better interaction and loading of lipophilic drugs such as ITZ. Recent research has also validated the advantages of PCL in topical drug delivery systems, including a marked improvement in skin retention and antifungal efficacy compared to traditional formulations, protection

against ITZ degradation in the environment, and enhanced local bioavailability following PCL carrier encapsulation, and the ability to alter the surface to improve targeting and release profiles [38].

PLGA is another FDA-approved polymer used extensively in drug delivery, especially as nanoparticles, because of its controllable biodegradation rate that can be modulated by varying the ratio of lactic acid to glycolic acid. PLGA has good safety profiles and has been included in several marketed formulations; however, its slightly faster degradation compared to PCL may sometimes limit its use for long-term delivery applications, and its acidic degradation products can cause local irritation or destabilization pH-sensitive drugs [39].

These disadvantages notwithstanding, PLGA remains a popular choice for systemic drug delivery (particularly parenteral administration) because of its inherent flexibility; it can be used to fabricate in situ-forming implants, microspheres, and targeted nanoparticles. However, PCL may provide a better option for long-term topical applications that require prolonged release with minimal irritation. Chitosan is an interesting polysaccharide naturally obtained from the chitin of crustaceans; it is known for its mucoadhesive properties and capacity to open tight junctions in epithelial tissues facilitating paracellular drug transport [40].

It has especially been shown to be effective in transmucosal and topical drug delivery; for example, it has been used in the development of antifungal delivery systems because chitosan nanoparticles can be bioadhesive and enhance penetration [41], but they suffer from poor mechanical strength, batch-to-batch variability, instability at low pH, their cationic nature leading to electrostatic interactions with negatively charged biological membranes that may increase initial adhesion, but often leads to cytotoxicity or inflammation with longer exposure time, and the environmental factors affecting stability of chitosan nanoparticles, such as pH and ionic strength. Of these three systems for Itraconazole delivery, PCL is a better choice due to its compatibility with hydrophobic drugs, longer release kinetics, physicochemical stability, and the fact that it does not produce acidic degradation byproducts (unlike PLGA) which can destabilize sensitive APIs; in addition, PCL

offers more formulation flexibility than chitosan because of pH sensitivity and lack of structural robustness.

In recent studies, nanoparticles made from PCL with or without surface modifiers or embedded into gels have been shown to increase skin permeation while minimizing systemic exposure; hence they are a promising option for transdermal delivery of ITZ in the treatment of superficial and cutaneous fungal infections [11] [42]. PCL is the most balanced polymer for the sustained, stable, and effective delivery of Itraconazole in nanocarrier systems.

2.5 Functional Role of Poloxamer 407 in Nanoparticle Systems

Poloxamer 407, or Pluronic F127, is an amphiphilic nonionic triblock copolymer of poly (ethylene oxide)-poly (propylene oxide)-poly (ethylene oxide) (PEO-PPO-PEO), which has attracted much attention in pharmaceutical formulation science because it exhibits thermoresponsive behaviour and good biocompatibility. Poloxamer 407 can be used as a steric stabilizer for nanoparticles, adsorbing onto the surface of polymeric nanoparticles to form a hydrophilic corona that prevents aggregation by steric hindrance. This stabilization ensures long-term colloidal stability and uniform particle size distribution, which is critical for reproducible and consistent drug release. Poloxamer 407 is amphiphilic, thermoresponsive, and biocompatible; thus, it has received considerable interest in pharmaceutical formulation science as a steric stabilizer that can increase the solubility of hydrophobic agents (e.g., G. modulating drug release, and Itraconazole [ITZ]) [43].

Another important role of Poloxamer 407 is the enhancement of skin permeation as a result of its surfactant-like behaviour, which allows it to temporarily disrupt the lipid structure of the stratum corneum and increase skin permeability [44]. Therefore, it is well suited for topical and transdermal formulations that need to deliver drugs with low skin permeability such as ITZ. Poloxamer 407 also exhibits

thermoresponsive gelation at specific concentrations; when prepared as a solution, the material is free flowing at lower temperatures but forms gels when heated to body temperature. This characteristic can be used to create in situ-forming gels, which increase the duration and retention of the drug at the application site by solidifying when applied to the skin for topical and transdermal application of poorly permeable medication formulations, including ITZ. Also, when prepared in solution, it retains its liquid form until heated to body temperature; upon heating to body temperature, the gel becomes solid (a process called thermoresponsive gelation), enabling the creation of in situ-forming gels that harden after application to the skin and extend the period of residence and drug retention at the site of administration. Poloxamer 407 has proven efficacy as a co-solvent for orally delivered poorly permeable drugs, and is also effective in topical preparations of poorly permeable drugs [45]. Additionally, Poloxamer 407 has been used to produce multifunctional nanogels when combined with polymers like PCL and bioadhesive agents such as Carbopol 934; these hybrid systems exploit Poloxamer solubilizing and gelling properties, PCL's controlled-release matrix, and the bioadhesive nature of Carbopol to develop a transdermal drug delivery platform that can significantly increase local drug concentration, reduce systemic side effects, and enhance therapeutic outcomes in the treatment of dermal fungal infections. Poloxamer 407 is also used as an important excipient in nanomedicine because it can enhance solubility and dispersion of nanoparticles, stabilize hydrophobic nanoparticles, promote skin penetration, and provide thermoresponsive gelling properties to formulate sophisticated topical and transdermal drug delivery systems for poorly soluble antifungal drugs such as Itraconazole [46].

2.6 Carbopol 934 in Nanogel Formulations: Enhancing Bioadhesion and Controlled Release

Carbopol 934 is a high molecular weight cross-linked polyacrylic acid polymer that is widely used as an excipient due to its mucoadhesive, thickening, and gel-forming properties; it can improve the performance of topical and transdermal drug

delivery systems, especially in nanogel formulations for localized and sustained drug release [47].

Carbopol 934 also functions as a gelling agent and aids nanoparticle stability and uniform distribution within the formulation; its high swelling capacity in aqueous media enables entrapment and immobilization of drug-loaded nanoparticles and provides a sustained-release profile, while pH sensitivity promotes site-specific drug release for fungal infections [48].

One advantage of using gels based on Carbopol is their strong ability to form hydrogen bonds with biological tissues; this increases the adhesive interaction between nanogel and skin or mucosal surfaces, thus prolonging the residence time of a drug for better bioavailability and minimizing wash-off due to perspiration or movement. The prolonged contact of the infected area in treatment of dermal fungal infections is a good application where Carbopol-based gels can be used as they increase the adhesion of the nanogel with skin or mucosal surfaces.

Carbopol 934 has ability to improve the sol-gel transition and mucoadhesion properties of the composite systems for longer residence at the application site, controlled drug release, and improved patient compliance when combined with other excipients, such as Poloxamer 407, to create thermoresponsive, bioadhesive nanogels [49]. The addition of Carbopol 934 to nanogels has been found to enhance the penetration and retention of antifungal agents on the skin; also allows for formulations with desired rheological properties, which are required for spreadability, patient acceptability, and application ease. The ability of Carbopol to create a hydrophilic environment helps in solubilization of hydrophobic drugs such as Itraconazole [50].

Carbopol 934 is an important part of transdermal delivery systems based on nanogel. It has various functions in gel formation, stabilization of nanoparticles, bioadhesion, and controlled drug release greatly improve topical antifungal formulations and therapeutic efficacy. It provides a strong platform for resolving the biopharmaceutical issues related to Itraconazole when combined with other polymers [51].

2.7 Transdermal Nanogels: A Hybrid System for Localized and Sustained Delivery

Topical drug delivery has the potential to deliver poorly soluble antifungal agents such as Itraconazole for localized fungal infections including dermatophytosis, fungal keratitis, and onychomycosis; however, traditional topical vehicles (e.g., ointments, creams, lotions) are limited by poor permeation of drug, a greasy texture, and reduced retention time at the site of application, and instability under different environmental conditions.

The combination of nanotechnology with gel-based systems for drug delivery has emerged as an interesting approach to overcome some drawbacks associated with conventional topical vehicles; these novel drug carriers known as transdermal nanogels offer enhanced mechanical strength, improved spreadability, increased adherence to skin surface (longer residence time), and sustained release of drugs at the target site [52].

The encapsulated drug particles have a nanoscale dimension that allows for deeper skin penetration through the intercellular or transappendageal pathways, which is further facilitated by the gel matrix retaining the nanoparticles at the application site and acting as a reservoir for gradual release into the deeper dermal layers [53].

In addition, they have good biocompatibility, ease of use, and patient acceptance; they are non-invasive and painless alternatives to systemic administration, minimizing gastrointestinal side effects, first-pass metabolism, and systemic toxicity commonly associated with oral Itraconazole.

The rheological and physicochemical properties of nanogels can be tuned by altering the type of polymer, the surface charge on the nanoparticle, and crosslinking density to address various severities of infection and skin types [54]. In general, transdermal nanogel delivery systems offer a multimodal platform for localized delivery with sustained antifungal action that is well suited for conditions where prolonged exposure and penetration through keratinized tissues are needed.

2.8 Recent Advances and Formulation Gaps

The use of nanotechnology-based delivery systems to increase solubility and bioavailability of poorly soluble drugs is a growing trend in pharmaceutical science because it also improves patient compliance and reduces toxicity, but many of these formulations fail at clinical translation or during scale-up, as well as achieving consistent therapeutic efficacy across different patient populations [55].

Preclinical studies with poorly soluble drugs have shown that they can enhance solubility, bioavailability, compliance, and toxicity, but many of these formulations fail during clinical translation, scale-up, or achieve consistent therapeutic efficacy across patient populations. Our findings demonstrated that ITZ-loaded lipid nanocapsules (LNCs) can improve the performance of ITZ delivery still encounters significant biopharmaceutical challenges and requires deep skin penetration, prolonged retention, and targeted delivery, which are difficult to achieve with conventional oral and topical systems.

Thus, the last decade has witnessed a shift toward the incorporation of lipids, polymers, and nanocarriers into advanced drug delivery systems like SLNs, NLCs, micelles, and nanogels; each iteration has sought to overcome one or more shortcomings of earlier systems [56]. However, the development pipeline highlights significant unmet needs; for example, SLNs are beneficial in improving stability but suffer from burst release and poor skin penetration; nanosuspensions have potential for rapid dissolution but do not hold well during storage; polymeric micelles demonstrate enhanced oral bioavailability but cannot be used for site-specific dermal delivery; liposomes and NLCs increase patient compliance and dermal drug release, but they do not offer the best retention or scale-up [57]. Among promising platforms, emerging hybrid nanogels (especially those integrating PCL, Poloxamer 407, and Carbopol 934) are being developed due to their synergistic benefits such as sustained drug release with good retention, high mechanical stability, and compatibility with a variety of antifungal APIs; however, they are underexplored in clinical settings and need extensive optimization for human application. In this section, the major advances in ITZ formulations are briefly summarized in Table

2.1, including key innovation and prevailing limitation of each platform, with an intent to identify persistent gaps and establish rationale for new hybrid systems that can overcome previous constraints.

TABLE 2.1: Summary of Itraconazole Formulation Studies in the Last Decade

Formulation Type	**Objective**	**Key Findings**
Lipomer (polymeric lipid hybrid nanoparticles)	To optimize ITZ delivery via lipid-based nanocarriers	Improved solubility and sustained release using Box-Behnken design [58]
Microemulsion	To enhance skin penetration of ITZ for topical use	Effective drug release and patient-compliant formulation [59]
PLGA nanoparticles stabilized by vitamin-E TPGS	To increase antifungal efficacy and stability	Achieved high encapsulation efficiency and prolonged release [60]
Polymeric nanoparticle dermal gel	Develop ITZ dermal gel using nanoparticle encapsulation	Improved antifungal efficacy through skin-targeted delivery [61]
Nanoemulsion gel	To design a novel transdermal ITZ formulation	Achieved effective skin permeation and antifungal action [62]
Chitosan hydrogel with ITZ-curcumin	Treatment of onychomycosis (nail fungal infection)	Dual-drug system showed enhanced efficacy and nail bed penetration [63]
Electrospun nanofibers	Topical ocular delivery system for sustained ITZ release	Demonstrated controlled release with potential for eye infection therapy [64]
Nanoemulgel	ITZ topical formulation for efficient fungal treatment	Demonstrated high skin retention and permeation [65]
Lipid nanoparticles	Evaluate skin targeting and antifungal efficacy	Achieved superior skin localization and treatment outcome [66]

This review highlights that while major strides have been made in using lipid-based and polymeric nanocarriers for Itraconazole delivery, persistent challenges remain in clinical translation, skin targeting, and formulation scale-up.

As newer hybrid systems like PCL-Poloxamer-Carbopol gels show promising preclinical results, future research should aim to bridge the gap between laboratory efficacy and real-world usability.

2.9 Problem Statement, Novelty and Rationale of the Present Work

The current investigation addresses a critical void in Itraconazole (ITZ) delivery by formulating a hybrid nanogel system designed for transdermal application.

Drawing from the decade-long evolution of ITZ formulations, it is evident that individual delivery systems—be it SLNs, liposomes, or polymeric micelles—are limited by one or more of the following: instability, insufficient dermal penetration, burst release, or patient non-compliance [11][67].

Despite encouraging outcomes with PCL nanoparticles, Poloxamer 407-based dispersions, and Carbopol-integrated gels, no single system has thus far succeeded in offering synergistic enhancement across all major pharmaceutical parameters: solubility, controlled release, dermal retention, biocompatibility, and patient-friendly application [68].

This study suggests a new combination of polycaprolactone (PCL) nanoparticles for sustained release, Poloxamer 407 for nanoparticle stabilization and skin permeation, and Carbopol 934 as a gel-forming agent with enhanced mucoadhesive and rheological properties, based on preclinical evidence that each component enhances dermal delivery of poorly water-soluble antifungal agents, as well as the formulation's hypothesized nanometric size range supports stratum corneum penetration without excessive systemic absorption—appropriate for topical fungal infections such as dermatophytosis, onychomycosis, and superficial candidiasis [69].

This study also assess optimized formulation for entrapment efficiency, particle size, polydispersity index, zeta potential, in vitro drug release kinetics, and ex vivo skin permeation and retention compared to conventional ITZ formulations to demonstrate superior characteristics.

In this regard, the current study not only introduces a novel hybrid delivery platform but also seeks to establish a clinically relevant and patient-friendly model of antifungal nanotherapy that addresses an unmet need from previous approaches. The purpose is to evaluate optimized formulation for key parameters such as entrapment efficiency, particle size, polydispersity index, zeta potential, in vitro drug release kinetics, and ex vivo skin permeation and retention compared with conventional ITZ formulations to demonstrate comparative superiority.

In doing so, the current research not only proposes an innovative hybrid delivery platform but also aims to establish a scalable and patient-compliant model of antifungal nanotherapy that addresses an unmet need from previous approaches

Chapter 3

Materials and Methods

3.1 Materials

USP-grade ITZ was generously provided by Vision Pharma (Islamabad, Pakistan).

Poloxamer 407 (a purified non-ionic surfactant) was obtained from Sigma-Aldrich (CHEMEI GmbH, Germany),

Polycaprolactone (PCL, average Mn ∼14,000 g/mol) was procured from Macklin Biochemical Co., Ltd. (CH1002, China).

Carbopol 934 was sourced from Spectrum Chemical Mfg. Corp. (USA).

Dimethyl sulfoxide (DMSO), eucalyptus oil, and triethanolamine (TEA, $\geq 99\%$, analytical grade were purchased from BioShop Canada Inc.

Methanol, disodium hydrogen phosphate, sodium chloride, and glycerin (99%, USP grade) were supplied by Merck.

Freshly distilled water was prepared in-house at the Faculty of Pharmacy, Capital University of Science and Technology (CUST), Islamabad.

3.2 Method

The nanoparticles were prepared using an optimized modified nanoprecipitation with control of critical process parameter as shown in Figure 3.1. For the organic phase preparation, PCL was initially dissolved in DMSO under magnetic stirring at 500 rpm and 25°C. Complete polymer dissolution was achieved through bath sonication at 30°C for 15 minutes.

For drug-loaded formulations, 10 mg of ITZ was gradually added to the PCL solution with continuous stirring at 800 rpm and maintained at 35°C for 15 minutes. The aqueous phase was prepared by dissolving Poloxamer 407 (2% w/v) in Distilled water.

Nanoparticle synthesis was performed by injecting the organic phase into the aqueous phase using a 22G needle at 0.25 mL/min. The injection process was conducted under constant homogenization at 2000 rpm using an overhead homogenizer. The resulting nanoparticle suspension was subjected to centrifugation (2000×g for 60 min at 25°C).

The pellet was washed twice with 5 mL cold distilled water followed by 1 minute of bath sonication. The purified nanoparticles were frozen at -20°C for 8 hours before lyophilization in a freeze dryer.

The lyophilization protocol consisted of primary drying at -40°C and 0.1 mbar for 12 hours followed by secondary drying at 25°C and 0.01 mbar for an additional 12 hours [70][71]. Different formulations were prepared by varying quantity of Polymer, surfactant and volume of aqueous phase as given in Table 3.1.

The gel matrix was prepared using a controlled hydration method to ensure optimal polymer dispersion. Carbopol 934 (1% w/v) was gradually sprinkled into ice-cold distilled water under constant stirring at 2000 rpm using an overhead stirrer. The acidic polymer dispersion was then neutralized using triethanolamine (TEA, 0.5% v/v) added drop wise (0.1 mL/min) from a calibrated burette while monitoring pH with a calibrated pH meter[72].

Table 3.1: Composition of Itraconazole-Loaded Polycaprolactone Nanoparticle Formulations

Formulation	Polymeric Phase			Aqueous Phase	Aqueous Phase
	ITZ (mg)	Polymer PCL (mg)	Solvent DMSO (mL)	Poloxamer 407 (%)	Volume (mL)
F1	10	20	10	2	10
F2	10	40	10	2	10
F3	10	60	10	2	10
F4	10	80	10	2	10
F5	10	20	10	1.0	10
F6	10	20	10	3.0	10
F7	10	20	10	5.0	10
F8	10	20	10	2.0	20
F9	10	20	10	2.0	30
F10	10	20	10	2.0	40

The neutralization process continued until reaching the target pH range of 5.5-6.0, which is compatible with the skin.

Following neutralization, the gel was subjected to a maturation period of 24 hours at 4°C to achieve complete polymer swelling and uniform viscosity. Eucalyptus oil was then incorporated as a permeation enhancer. Added one drop Eucalyptus oil and mixed thoroughly.

The lyophilized ITZ-loaded PCL nanoparticles were redispersed in glycerin (5% v/v) using bath sonication until achieving a homogeneous suspension. This nanoparticle-glycerin premix was then slowly incorporated into the gel base at a rate of 0.5 mL/min using a syringe while maintaining gentle magnetic stirring (300 rpm) at 25±0.5°C.

The mixing continued for an additional 30 minutes after complete addition to ensure uniform nanoparticle distribution without aggregation [65]

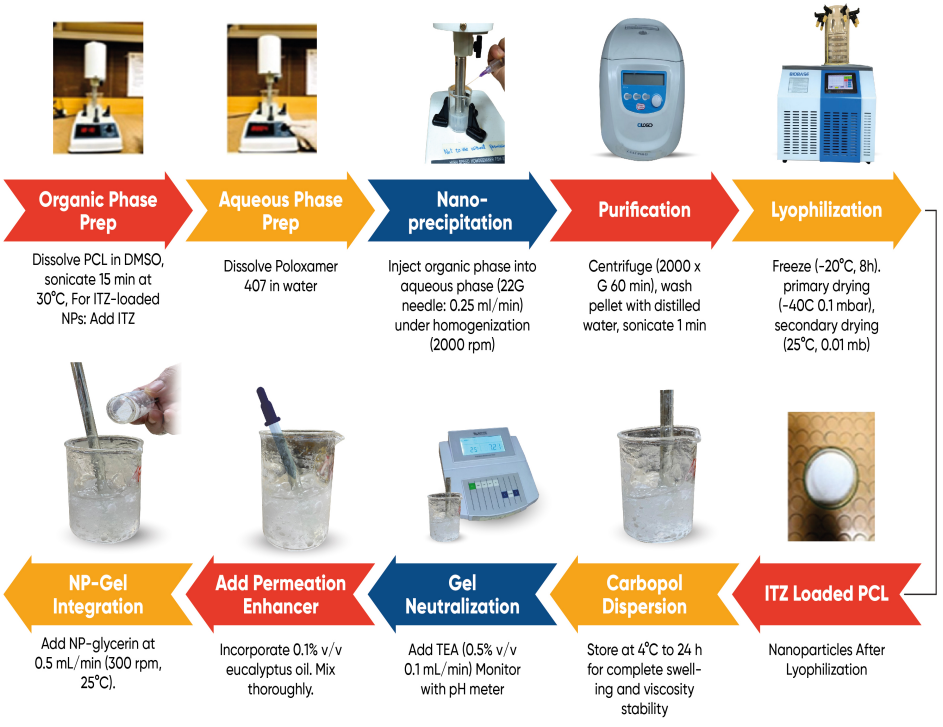

FIGURE 3.1: Schematic Diagram of the Nanoprecipitation Method for ITZ-PCL Nanoparticle Preparation

3.3 Characterization

3.3.1 Encapsulation Efficiency Determination

The encapsulation efficiency (EE) of Itraconazole-loaded nanoparticles was determined by indirect quantification. After nanoparticle preparation, the dispersion was centrifuged at 2000×g for 60 minutes at 25°C (Thermo Scientific, USA) to sediment the polymeric nanoparticles and to separate the free (unencapsulated) drug present in the aqueous supernatant. The clear supernatant was carefully withdrawn and analyzed spectrophotometrically using a UV–Visible spectrophotometer (Shimadzu UV-1800, Japan) at a λmax of 262 nm, which corresponds to the maximum absorbance of ITZ in the selected solvent system [73]. The encapsulation efficiency was then calculated using the equation 3.1

$$\text{Encapsulation Efficiency (\%EE)} = \left(\frac{W_{\text{total}} - W_{\text{free}}}{W_{\text{total}}} \right) \times 100 \tag{3.1}$$

Where:

W_{total}= Total amount of drug initially added during nanoparticle formulation

W_{free}= Amount of free (unencapsulated) drug found in the supernatant after centrifugation [74]

3.3.2 In Vitro Drug Release Study

The in vitro release behaviour of nanoparticles loaded with ITZ was assessed using a USP Type II (paddle) dissolution apparatus under controlled sink conditions. For the simulation of the sustained release environment, nanoparticles were encapsulated in pre-soaked dialysis membrane bags (MWCO 12-14 kDa) that allowed for selective drug diffusion and retained nanoparticles. Dissolution studies have been performed in two media, phosphate buffer (pH 7.4) and acetate buffer (pH 5.5). In order to improve the solubility of ITZ due to its poor water solubility

profile, sodium lauryl sulphate (SLS) 0.5% w/v was added to each buffer [75] . For physiological simulation, the volume of buffer solution in each vessel was kept at 500 mL and the rotating paddle was set at 100 rpm to ensure uniform mixing. At predetermined time intervals (0.5, 1, 2, 3, 4, 6, 8, 12, 18, and 24 hours), 2 mL samples were withdrawn and replaced immediately with equal volumes of fresh preheated medium to maintain both constant volume and sink conditions. The withdrawn aliquots were filtered through membrane filters at a pressure of 0.45 mmol membrane filter to remove any particulate matter and residues from the membrane. The concentration of ITZ in each sample was measured using a UV spectrophotometer at 262 nm using standard calibration curve [76] . The cumulative percentage of drug release was calculated and plotted as a function of time.

Dissolution data were fitted into various mathematical models, including zero-order, first-order, Higuchi, and Korsmeyer-Peppas models. The best fit was determined by comparing the correlation coefficients (R^2) of each of the two models, while the release exponent (n) of the Korsmeyer-Peppas equation provided an insight into the mechanism of drug release, distinguishing between Fickian diffusion, anomalous transport or case-II relaxation. All measurements were performed in triplicate and the results were expressed as mean ± standard deviation to ensure statistical robustness [77].

3.3.3 Swelling Behaviour

The swelling behaviour of Itraconazole-loaded PCL-Poloxamer nanoparticles was assessed to evaluate their ability to absorb fluid and their potential impact on the drug release kinetics. Accurately weighed dried nanoparticle samples (20 mg) were immersed in phosphate-buffered saline (PBS) at pH 7.4 and pH 5.5 to simulate physiological and skin surface conditions, respectively.

Samples were incubated at 37 ± 0.5 °C under mild agitation. At predefined time intervals (1, 3, 6, 12, and 24 hours), the swollen nanoparticles were gently removed,

surface moisture was blotted using filter paper to remove excess buffer, and the samples were reweighed. All measurements were performed in triplicate [78][79]. The swelling capacity (%) was calculated using the following equation 3.2

$$\text{Swelling Capacity (\%)} = \left(\frac{W_2 - W_1}{W_1}\right) \times 100 \tag{3.2}$$

Where:

W_1 = Initial dry weight of nanoparticles,

W_2 = Weight of swollen nanoparticles after excess buffer removal

3.3.4 Determination of Particle Size and Poly Dispersity Index

The particle size (Z-average) and the PI (polydispersity index) of the ITZ-NP were determined by dynamic light scattering (DLS) using the Zetasizer Nano ZS (Malvern Instruments, UK).

The samples were diluted 1:20 (v and v) with 2% (w/v) of Poloxamer 407 solution. The measurements were made at 25°C with a backscatter detection angle of 173° and each sample was analysed in three steps[80].

3.3.5 Surface Morphology

The morphological properties of ITZ-NP have been assessed by using field-emission scanning electron microscopy (FE-SEM; JSM-7900F, JEOL Ltd., Japan). A 10 μL aliquot of nanoparticle suspension was deposited on aluminium foil, air-dried at 25 ± 2°C and mounted on aluminium strata by a conductive carbon fibre tape.

The samples were sputtered with a 3nm gold- palladium thickened veil to increase the conductivity. The imaging was carried out at a voltage of 5-10 kV and a working distance of 5–10 mm[81].

3.3.6 Thermo Gravimetric Analysis/Differential Scanning Calorimetry

The thermal behaviour of lyophilized ITZ-NPs was investigated using simultaneous differential scanning Calorimetry thermogravimetric analysis (DSC-TGA; SDT Q600, TA Instruments).

Approximately 5–10 mg of sample was sealed in aluminium crucibles and heated from 25°C to 300°C at 10°C/min under nitrogen purge (50 mL/min). Thermal events (glass transition Tg, melting Tm, decomposition) were analyzed using TA Universal Analysis software[82].

3.3.7 Fourier-Transform Infrared Spectroscopy

The molecular interactions between ITZ and the polymer compounds were evaluated by the FTIR (Spectrum Two, PerkinElmer) in the range of 4000–400 cm^{-1}. The samples were prepared as potassium bromide (KBr) pellets (1:100 sample: KBr) and scanned with a resolution of 4 cm^{-1} with 32 accumulations.

The background correction was made using pure KBr. Characteristic functional group vibrations were compared between pure components and nanoparticles to determine potential drug-polymer interactions [83]

3.3.8 X-ray Diffraction

Crystallinity of Itraconazole in nanoparticle formulation was assessed with a Cu-K irradiation source (λ = 1.5406, 40 kV, 30 mA) using a X-ray Diffractometer (Scintag XGEN-4000, Advanced Diffraction System, Scintag Inc., USA). Samples were placed in a zero-background silicon holder and scanned over a 2θ range of 4–50° at a scan rate of 2°/min with a step size of 0.02°. Diffraction patterns were collected in continuous scan mode and analyzed using Scintag DataScan (v4.0) software [84].

3.3.9 Physical Parameters of Prepared Formulations Gel

The optimized nanoparticle formulation has been incorporated in a gel matrix of Carbopol 934 (1.0% w/w) to enhance topical delivery of the drug. The resulting formulations have been rigorously assessed for critical quality characteristics by means of a comprehensive physical characterization.

Macroscopic and organoleptic properties, pH determination, and rheological analysis The Formulations were visually checked for colour, clarity, and homogeneity and phase separation under ambient conditions. The pH of the surface was determined in three times by calibration calibrated digital pH meter (PHS-25CW, BANTE Instruments, China) at 25 ± 1°C. Prior to measurements, the instrument was standardized with buffer solutions of pH 4.0, 7.0 and 10.0. The electrode was allowed to be equilibrated with the sample for 30 seconds before recording to ensure accuracy and reproducibility. The viscosity profiles were evaluated using the Brookfield DV2T, which was equipped with a Spindle S64 memory card. The measurements were made at 25 ± 0.5 degrees Celsius over a range of gradient from 0.1 to 1.5 degrees Celsius. The usefulness of remission was assessed using a modified standardized method for remission of a candle. Approximately 350 mg of gel was placed in the centre of the glass plate ($10x5cm$) and a second glass plate of the same size and weight (5.8 ± 0.1 g) was dropped freely from a height of 5 cm. After 1 minute, the average diameter of the diffusion surface was measured in centimeters [85].

3.3.10 Ex Vivo Skin Permeation Studies

To assess the potential of the optimized nanoparticle formulation for transdermal application, penetration studies using Franz-diffusion cells and excreted intra-abdominal skin from healthy New Zealand white rabbits were carried out in vivo. Two gel formulations were evaluated: F2 Gel: Itraconazole-loaded PCL nanoparticle incorporated gel Plain Gel: Gel containing free Itraconazole. Full-thickness rabbit skin was excised, cleaned to remove subcutaneous fat, and equilibrated in

phosphate-buffered saline (PBS, pH 7.4) for 1 hour. The skin samples were then stored at 20°C and melted down before use [86].

Each skin sample was inserted between the donor and receptor compartment of the Franz diffusion cell (diffusion area = 2.54 cm 2) so that the stratum corneum is parallel to the donor side. The receptor compartment was filled with 20 mL of PBS (pH 5.5, to mimic skin surface conditions), maintained at 37±0.5°C and stirred continuously with a magnetic stirrer at a speed of 600 rpm. An accurately weighed amount (1g) of either F2 gel or plain gel was applied uniformly to the donor compartment.

At specific intervals (0.5, 1, 2, 6, 8, 12 and 24 h), 2 mL samples were taken from the receptor compartment and replaced by the same volume of fresh PBS to ensure that the saturation conditions were maintained.

The amount of the drug per square meter ($\mu g/cm^2$) was plotted against the time elapsed to obtain a permeability profile [87]. From the linear portion of the curve (steady state), the steady-state flux (Jss) was calculated from equation 3.3

$$J_{ss} = \frac{\Delta Q}{A\,\Delta t} \tag{3.3}$$

ΔQ = amount of drug permeated during steady state (μg)

A = effective diffusion area (2.54 cm^2)

Δt = time interval during steady-state linear region (h)

To compare permeation enhancement, the Enhancement Ratio (ER) was calculated from equation 3.4

$$\text{ER} = \frac{J_{\text{ss (F2 gel)}}}{J_{\text{ss (Plain gel)}}} \tag{3.4}$$

All experiments were conducted in triplicate (n = 3). Data are expressed as mean ± standard deviation (SD). An unpaired two-tailed Student's t-test was used to determine statistical significance, with $p < 0.05$ considered significant.

3.3.11 Skin Irritation Test

The dermal biocompatibility of nanogel loaded with ITZ was assessed in vivo in healthy adult New Zealand white rabbits (Oryctolagus cuniculus, n = 9) in accordance with OECD Guideline 404 and approved by the Institutional Animal Ethics Committee (EPC). Animals were randomly divided into three groups (n = 3 per group):

Test group: ITZ-loaded nanogel

Positive control: 0.8% w/v sodium lauryl sulfate (SLS) solution

Negative control: Untreated site (baseline skin response)

All animals were kept in a controlled environment (22 ± 2°C, 55 ± 5% RH, 12 h light/dark cycle) with unrestricted access to standard food and water for 48 hours. Prior to the experiment, the dorsal surface was carefully shaved with an electric clipper 24 hours prior to administration to avoid microscopic damage.

A 1 cm^2 test area was demarcated on each rabbit. Each formulation (0.1 g) was applied to the designated area using a sterile polypropylene spatula under an occlusive patch.

Observations were made during the initial 4 hours and at 24 h, 48 h, and 72 h post-application for signs of erythema, edema, and behavioural responses such as scratching or discomfort. The Draize scoring system was used to quantify the severity of erythema and edema:

0 = None

1 = Mild (faint or light pink coloration, <1/3 area)

2 = Moderate (definite erythema, 1/3–2/3 area)

3 = Severe (dark red, >2/3 area or spreading beyond site)

The Primary Irritation Index (PII) was calculated 72 hours using the Equation 3.5

$$\text{PII} = \frac{\sum(\text{erythema score} + \text{edema score at 72 h})}{\text{number of animals}} \tag{3.5}$$

Based on OECD classification, PII < 0.5 is considered non-irritant [88].

3.3.12 Stability Study

The physical stability of the selected gel formulations has been assessed under standardized storage conditions in accordance with the ICH guidelines. The samples were packed in light-resistant containers (glass bottles with aluminium foil lining) and stored under three different environmental conditions: 4 ± 1°C (refrigerated), 25 ± 2°C (ambient), and 40 ± 2°C/75 ± 5% RH (accelerated), respectively. The acceptance criteria for physical stability included maintaining a homogenous appearance, viscosity at a level of at least 10 percent and pH stability (calibration of pH by a calibrated pH meter) at predetermined intervals (0, 1, 2 and 3 months, formulations were evaluated for:

1. Visual characteristics (color, homogeneity, phase separation)

2. pH stability (using calibrated pH meter)

3. Rheological properties (viscosity measurements at controlled shear rates)

The acceptance criteria for physical stability included maintenance of homogeneous appearance, viscosity within ±10% of initial values, and pH stability within ±0.5 units [89].

3.3.13 Statistical Analysis

All data were analysed using SPSS Statistics 26.0 (IBM, USA). One-way analysis of variance (ANOVA) with Tukey's post hoc test was applied to compare means. A p-value <0.05 was considered statistically significant. Results are presented as mean ± SD ($n = 3$).

Chapter 4

Results and Discussion

4.1 Encapsulation efficiency

The encapsulation efficiency (EE) of ITZ-loaded PCL nanoparticles varied significantly across the prepared formulations, with values ranging from 70.2% to 88.4% ($p < 0.05$) as shown in Table 4.1. Among these, formulation F2 exhibited the highest EE of 88.4±1.2%, which was statistically superior to the other formulations, as confirmed by one-way ANOVA followed by Turkey's post-hoc test ($p < 0.05$). In the polymer content group (F1 to F4), increasing PCL concentration from 20 mg to 40 mg significantly improved EE from 78.2% to 88.4% ($p < 0.05$). However, further increases in PCL content to 60 mg (F3, 81.5±1.4%) and 80 mg (F4, 80.1±1.5%) resulted in a decline in EE compared to F2, with differences being statistically significant ($p < 0.05$), suggesting the existence of an optimal polymer concentration beyond which no additional encapsulation advantage is achieved [90]. In the surfactant concentration group (F5 to F7), EE was significantly affected by Poloxamer 407 content. A lower surfactant concentration (1%, F5) resulted in a reduced EE of 72.6±1.9%, which was significantly lower than F2 ($p < 0.05$).

Increasing Poloxamer 407 concentration to 3% (F6, 80.9±1.3%) and 5% (F7, 79.8±1.6%) improved EE compared to F5 but failed to reach the performance

of F2, with statistical differences remaining significant ($p < 0.05$) [91]. These findings indicate that 2% Poloxamer 407 represents an optimal concentration for achieving high encapsulation, likely due to an ideal balance between nanoparticle stabilization and prevention of drug leakage.

Among Formulations, F8 to F10, an inverse relationship between aqueous volume and EE was evident. Increasing the aqueous phase from 10 mL (F2, 88.4±1.2%) to 20 mL (F8, 76.8±1.5%), 30 mL (F9, 74.5±1.7%), and 40 mL (F10, 70.2±2.0%) resulted in a statistically significant decrease in EE ($p < 0.05$), likely due to enhanced drug diffusion into the aqueous phase during nanoparticle formation [92].

These systematic trends collectively demonstrate that formulation F2, containing 40 mg PCL, 2% Poloxamer 407, and 10mL aqueous phase, achieved the most favorable encapsulation efficiency, offering a statistically optimized system for effective ITZ encapsulation and stable nanoparticle formation [93].

TABLE 4.1: Encapsulation efficiency (EE) of ITZ-loaded PCL nanoparticle formulations (n=3).

Formulations	**Encapsulation Efficiency (EE, %)**
F1	78.2 ± 1.6
F2	85.4 ± 1.2
F3	81.5 ± 1.4
F4	80.1 ± 1.5
F5	72.6 ± 1.9
F6	80.9 ± 1.3
F7	79.8 ± 1.6
F8	76.8 ± 1.5
F9	74.5 ± 1.7
F10	70.2 ± 2.0

4.2 In-vitro Drug Release

The drug release behaviour of Itraconazole (ITZ)-loaded polycaprolactone (PCL) nanoparticles was systematically investigated under simulated skin surface (pH 5.5) and physiological (pH 7.4) conditions to elucidate the predominant release mechanisms and identify the most promising formulation. The cumulative drug release profiles for all formulations (F1–F9) are depicted in Figure 4.1, while corresponding release kinetic parameters derived from zero-order, first-order, Higuchi, and Korsmeyer–Peppas models are summarized in Table 4.2.

At pH 5.5, representing the mildly acidic environment of human skin, all formulations exhibited a sustained and controlled drug release profile over 24 hours. The predicted cumulative drug release at the end of 24 hours ranged from 62.0% ± 2.5% to 82.0% ± 3.2%, with statistically significant differences among the formulations ($p < 0.05$, one-way ANOVA followed by Tukey's post hoc test).

Notably, Formulation F2 exhibited the most favorable release profile, achieving the highest cumulative drug release of 82.0% ± 3.2%, which was significantly greater ($p < 0.05$) than all other tested formulations. Additionally, F2 demonstrated the strongest correlation with the Higuchi model ($R^2 = 0.9804$), confirming a robust diffusion-controlled release mechanism.

These results clearly indicate that F2 is the optimal formulation for achieving efficient drug release on the skin surface. Other formulations, including F3 (74.0% ± 2.8%), F5 (75.0% ± 3.1%), and F8 (73.0% ± 2.6%), showed moderate release profiles, while formulations F1, F4, F6, F7, and F9 exhibited comparatively lower cumulative drug release (62.0% to 70.0%) with no statistically significant differences within this group ($p > 0.05$).

Kinetic modelling confirmed that the Higuchi model, which describes diffusion-controlled drug release from a homogenous polymeric matrix, provided the best overall fit for most formulations at pH 5.5. Specifically, eight out of nine formulations exhibited strong linearity with R^2 values exceeding 0.91, indicating that Fickian diffusion was the dominant release mechanism under these conditions. The

superior fit of F2 further supports its favorable release behaviour and suggests effective diffusion of ITZ from the nanoparticulate matrix.

These findings align with previous studies demonstrating diffusion-dominated release from hydrophobic polymer matrices under mildly acidic, non-swelling conditions [94] [95].

The in-vitro release study demonstrated a pH-dependent release profile, with a cumulative drug release of 94.34% of F2 at pH 7.4 over 24 hours. The in-vitro release at pH 7.4 reached approximately 50% within 10 hours, followed by gradual release up to 80% by 24 hours. Formulations F2 and F3 showed the highest release rates, nearing 80% cumulative release. In contrast, F6-F9 exhibited slower release, plateauing around 60%.

This pH-dependent pattern suggests polymer swelling enhances drug diffusion under physiological conditions. Overall, the fit to the Higuchi model decreased for several formulations, with R^2 values falling below 0.70 for F4 ($R^2 = 0.6268$), F6 ($R^2 = 0.6679$), and F7 ($R^2 = 0.6685$), suggesting that additional mechanisms such as matrix swelling, relaxation, or erosion contribute to drug release under alkaline conditions, beyond pure diffusion [96].

At this pH, the Korsmeyer–Peppas model provided improved statistical performance, indicating a transition to anomalous (non-Fickian) release behaviour.

For instance, F9 exhibited a significantly better fit to the Korsmeyer–Peppas model ($R^2 = 0.8755$) compared to the Higuchi model ($R^2 = 0.7358, p < 0.05$), while F5 showed a similar trend (Korsmeyer–Peppas R^2= 0.7690, Higuchi $R^2 = 0.7049$). The corresponding n-values, all below 0.45, further confirm the involvement of complex release mechanisms, likely involving polymer relaxation and matrix erosion under physiological conditions [97].

Collectively, these findings demonstrate a statistically significant, pH-dependent release behaviour for ITZ-loaded nanoparticles. A Fickian, diffusion-dominated release profile was observed at pH 5.5, transitioning to anomalous, non-Fickian mechanisms at pH 7.4 ($p < 0.05$, based on comparative model fits and n-values).

Among all tested formulations, F2 emerged as the most promising candidate for dermal drug delivery, offering the highest drug release efficiency coupled with a robust diffusion-controlled release mechanism at the skin surface.

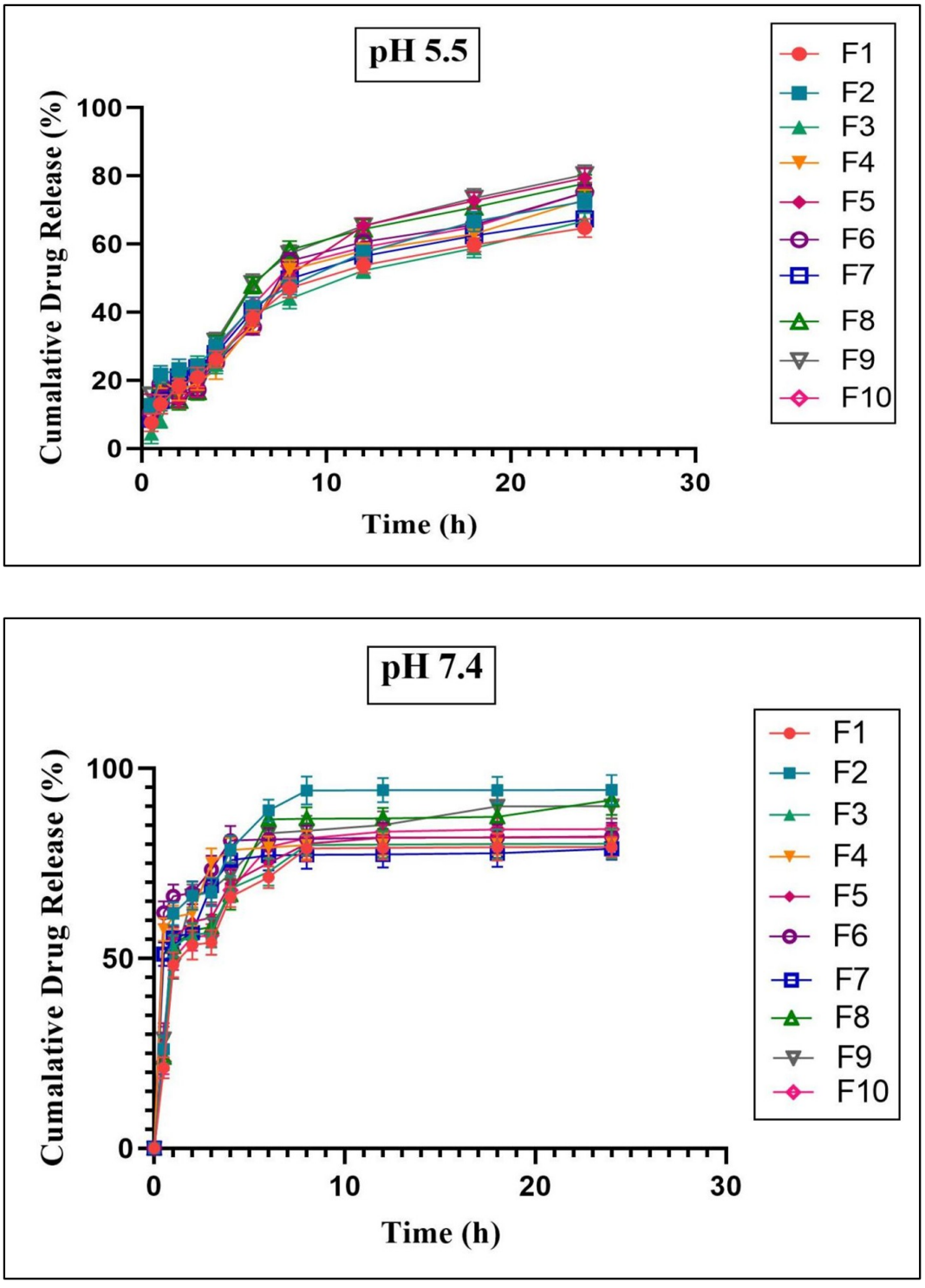

FIGURE 4.1: In Vitro, drug release kinetics of ITZ loaded PCL nanoparticles (F1-F10) in simulated skin pH 5.5 and at physiological pH 7.4. Cumulative release (%) was measured over 24 hours to evaluate pH-responsive behaviour for transdermal delivery applications.

TABLE 4.2: In vitro Drug Release Kinetic Models (Zero-order, First-order, Higuchi, Korsmeyer–Peppas) of ITZ loaded PCL nanoparticles (F1-F10) at pH 5.5 and 7.4

Sample	pH	Zero Order		First Order		Higuchi		Korsmeyer-Peppas R^2		
		R^2	K	R^2	K	R^2	K	R^2	K	n
F1	5.5	0.8691	4.2187	0.429	0.2987	0.9653	14.045	0.9318	21.7158	0.2683
	7.4	0.5154	8.7142	0.1822	0.3937	0.7125	29.483	0.721	67.2749	0.0043
F2	5.5	0.9206	4.4980	0.3817	0.3279	0.9804	16.450	0.969	22.1322	0.3307
	7.4	0.4853	10.6768	0.1689	0.4140	0.672	36.169	0.6998	82.1200	0.0011
F3	5.5	0.8682	4.2490	0.4358	0.2738	0.9681	13.842	0.9484	17.6730	0.3690
	7.4	0.5173	8.2470	0.1716	0.3994	0.7052	30.690	0.7171	69.1319	0.0046
F4	5.5	0.8929	4.0769	0.4386	0.3190	0.9389	14.964	0.9192	19.2977	0.3594
	7.4	0.3835	2.9964	0.1381	0.4093	0.6268	34.032	0.6345	74.5645	0.0040
F5	5.5	0.9165	3.4815	0.5198	0.3007	0.9565	14.791	0.9466	23.9848	0.2602
	7.4	0.5088	8.0624	0.1659	0.4022	0.7049	31.795	0.769	71.3336	0.0037
F6	5.5	0.8817	4.6930	0.4572	0.3195	0.936	14.994	0.9069	20.4550	0.3330
	7.4	0.389	2.9276	0.1331	0.4147	0.6679	35.391	0.4575	76.4040	0.0073
F7	5.5	0.8645	4.3338	0.4081	0.3052	0.9643	15.053	0.9358	23.7079	0.2563
	7.4	0.4163	3.6864	0.1486	0.4033	0.6685	32.120	0.5874	67.8528	0.0305
F8	5.5	0.8432	4.5586	0.4461	0.3253	0.919	16.127	0.8359	24.4698	0.2810
	7.4	0.5623	9.2102	0.1902	0.4012	0.7396	32.354	0.7077	63.1798	0.0915
F9	5.5	0.8672	3.4428	0.4647	0.3102	0.9388	16.002	0.8666	23.6103	0.3002
	7.4	0.5485	7.7592	0.1783	0.3979	0.7358	33.152	0.8755	66.8136	0.0715
F10	5.5	0.8879	4.6638	0.4246	0.3150	0.9666	15.672	0.9282	19.8883	0.3696
	7.4	0.5359	8.8423	0.185	0.3970	0.7237	30.880	0.7057	69.8522	0.111

4.3 Swelling Behaviour

The swelling dynamics of nanoparticles of Polycaprolactone (PCL) are of key importance in transdermal drug delivery systems, where controlled hydration controls the drug diffusion kinetics while preserving structural integrity at the skin interface.

Moderate swelling at skin pH (∼5.5) is necessary to increase the release of the drug by hydration-induced matrix relaxation without compromising the NP adhesion to the stratum corneum, a critical balance for a sustained transdermal delivery [98].

In this study, the pH-dependent swelling profiles were systematically assessed under physiological (pH 7.4) and simulated acidic (pH 5.5) conditions, as shown in Figure 4.2.

A one-way ANOVA with Tukey's post-hoc tests ($\alpha = 0.05$, n = 3) revealed a significant compositional effect on the equilibrium swelling ratios ($F(9, 40) = 28.6$, $p<0.001$), confirming that formulation design critically modifies hydration behaviour (Figure 4.2).

The formulation F2 (40 mg PCL, 2% Poloxamer 407) demonstrated an optimal swelling ratio of 1.42± 0.05 at pH 5.5 and 1.39 ± 0.04 at pH 7.4 resulting in a balance between hydration-induced drug release and mechanical stability. This controlled swelling is in line with the ideal ranges reported for transdermal systems where excessive hydration (>1.5) risks particle disintegration, while insufficient swelling (<1.3) limits the diffusion of the drug [13]. Increasing the concentration of the PCL from 20 mg (F1) to 40 mg (F2) considerably reduced the swelling by 6.4% ($p = 0.007$). Conversely, preparations with a higher content of Poloxamer 407 (e.g. F7: 5% surfactant) showed destabilizing swellings (1.563 ± 0.061 at pH 5.5; $p = 0.003$ vs. F2), consistent with surfactant-mediated micellization and pore formation. Increasing the aqueous phase volume from 10 mL (F2) to 40 mL (F10) reduced swelling ratios by 11.2% (1.248 ± 0.038; $p < 0.001$ vs. F2), attributed to diminished polymer packing density during nanoprecipitation. Despite this, pH

sensitivity (quantified as the % variation in swelling between pH 5.5 and 7.4) remained statistically constant across formulations (2.1% ; p = 0.22–0.48),suggesting that surface hydrophilicity is primarily regulated by the protonation of terminal carboxyl groups of the PCL (pKa) and not by the bulk matrix [99]. Notably, acidic skin pH (5.5) in all NPs induced an increase in swelling higher than physiological pH (7.4) in accordance with protonation-induced hydrophilic enhancement. This pH response is beneficial to the transdermal system, as localized swelling at the skin surface may increase the rate of drug release at the application site. Statistical analysis further showed that doubling the weight of PCL (20 to 40 mg) reduced the intra-group variability of swelling while increasing the structural destabilization of Poloxamer 407 from 2 to 5 % (F2). The robustness of the swelling profile of F2, combined with its pH tolerance, supports its selection as the preferred formulation for further characterization.

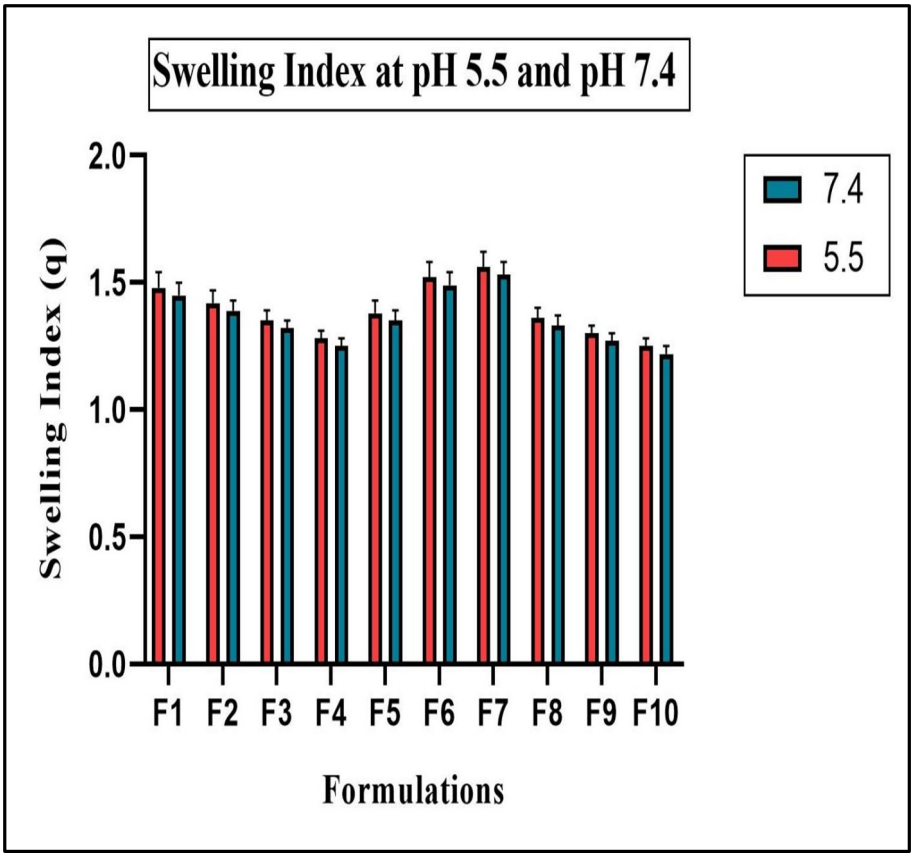

FIGURE 4.2: Swelling Index (q) of nanoparticle formulations (F1 to F10) at pH 5.5 and pH 7.4. Data are presented as mean ± SD (n = 3). Statistical significance was determined by one-way ANOVA with Tukey's post-hoc test (α = 0.05)

4.4 Particle Size, Polydispersity Index and Zeta Potential

The particle size and surface characteristics of nanoparticles are critical determinants of their performance, particularly for transdermal and topical drug delivery applications. In this study, dynamic light scattering (DLS) analysis revealed that the ITZ-loaded PCL nanoparticles (Formulation F2) exhibited a Z-average hydrodynamic diameter of 154.6 nm with a dominant peak at 118.9 nm (Figure 4.3). Nanoparticles within the size range of 100–200 nm are considered optimal for topical delivery, as they facilitate enhanced penetration into the stratum corneum and effective distribution within the viable epidermis, while minimizing the likelihood of systemic absorption [100].

The polydispersity index (PDI) of the formulation was recorded as 0.378, indicating a moderately narrow size distribution. While a PDI value below 0.3 is indicative of monodisperse systems, values between 0.3 and 0.5 are generally acceptable for polymeric nanoparticle formulations, especially those prepared by nanoprecipitation using amphiphilic stabilizers such as Poloxamer 407 [101].

The observed PDI reflects the controlled formulation parameters and efficient stabilization of nanoparticles, ensuring uniform particle size distribution, which is essential for consistent drug release and reproducible biological performance. The electrokinetic stability of the nanoparticles was assessed by zeta potential analysis, which showed a value of 10.7 ± 5.36 mV.

Although colloidal systems with zeta potential values exceeding ±30 mV are generally considered electrostatically stable, polymeric nanoparticle systems stabilized with non-ionic surfactants such as Poloxamer primarily rely on steric hindrance to prevent particle aggregation [102]. The slight negative surface charge observed in this study is attributed to the terminal carboxyl and ester functional groups present on the PCL chains, as well as the partial adsorption of the surfactant at the nanoparticle surface. This negative surface potential contributes to colloidal stability while minimizing the risk of aggregation during storage and application.

Furthermore, nanoparticles with lower surface charge have been associated with reduced skin irritation potential, an essential attribute for transdermal and topical formulations [103]. Overall, the combination of small particle size, acceptable size distribution, and sufficient colloidal stability confirm the suitability of the developed ITZ-loaded PCL nanoparticles for efficient and safe transdermal drug delivery.

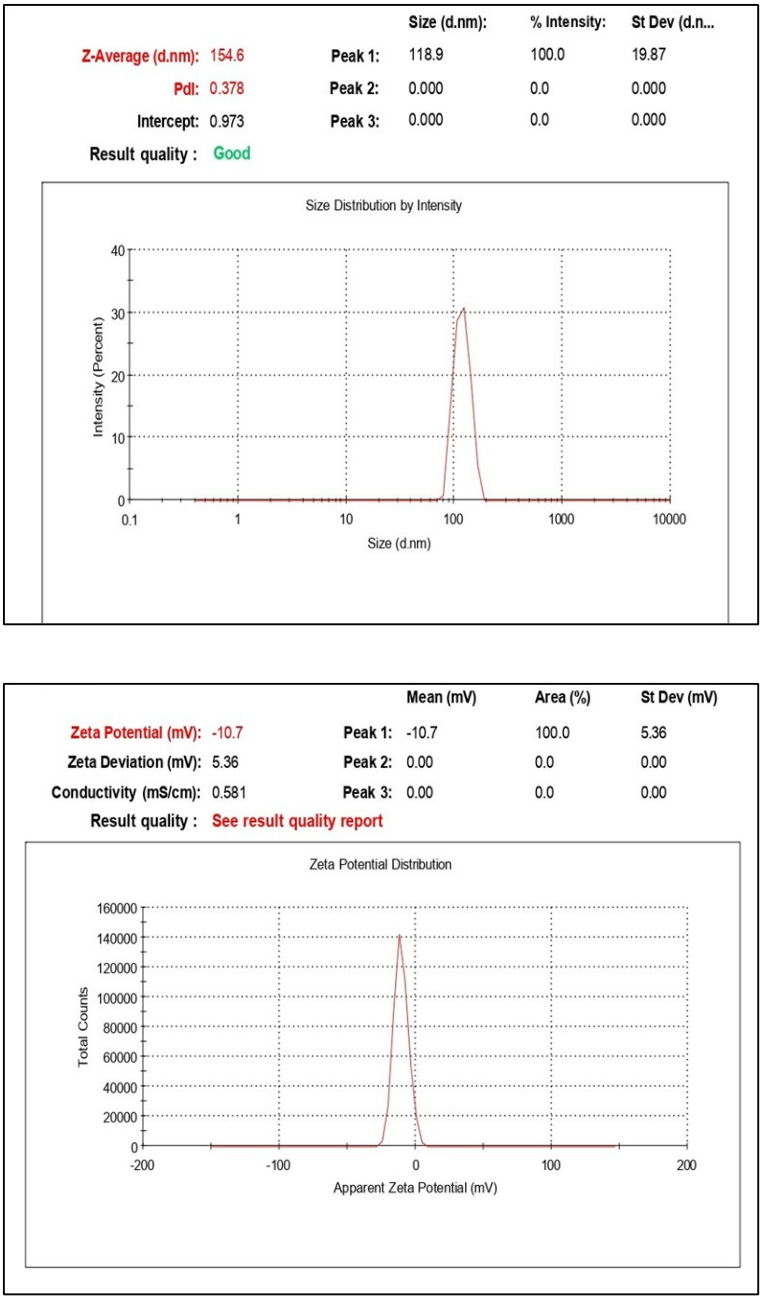

FIGURE 4.3: Particle size distribution and polydispersity index (PDI) of ITZ-loaded PCL nanoparticles determined by dynamic light scattering (DLS). The formulation exhibited a Z-average diameter of 154.6 nm with a PDI of 0.378, indicating moderate size uniformity

4.5 Scanning Electron Microscopy

The surface morphology and structural characteristics of the developed polycaprolactone (PCL) nanoparticles were investigated using Scanning Electron Microscopy (SEM), and the representative micrographs at different magnifications are presented in Figure 4.4. At lower magnifications (100× and 250×) (Figure 4.4), the nanoparticles appeared as agglomerated particulate clusters, which may be attributed to the hydrophobic nature of PCL and the lyophilization process that promotes particle aggregation. Such agglomeration is frequently reported for polymeric nanoparticles owing to weak van der Waals interactions and the absence of stabilizing agents on the particle surface [104]. With progressive magnification (500× to 5000×) (Figure 4.4), the micrographs revealed more detailed surface architecture of the nanoparticles.

The nanoparticles exhibited a distinct irregular, flake-like morphology with interconnected porous structures and surface roughness. The porous appearance and wrinkled texture can be attributed to solvent evaporation and polymer precipitation during nanoparticle formation via the emulsification-solvent evaporation technique. Such morphological features are desirable for enhancing the effective surface area, which can facilitate higher drug loading and sustained release profiles.

The pronounced porosity and interconnected voids observed at higher magnifications are indicative of the structural rearrangement of the PCL matrix during solvent removal. The presence of such porous networks is particularly advantageous for controlled drug delivery applications, as it can provide diffusion channels for drug molecules and contribute to prolonged release kinetics [105].

Furthermore, the irregular and rough surface morphology may enhance mucoadhesive or skin-interactive properties in topical or transdermal delivery applications, thereby improving drug permeation [106].

Overall, the SEM analysis confirmed the successful fabrication of PCL nanoparticles with characteristic porous, rough, and irregular morphology, consistent with the design objectives for controlled and sustained drug delivery.

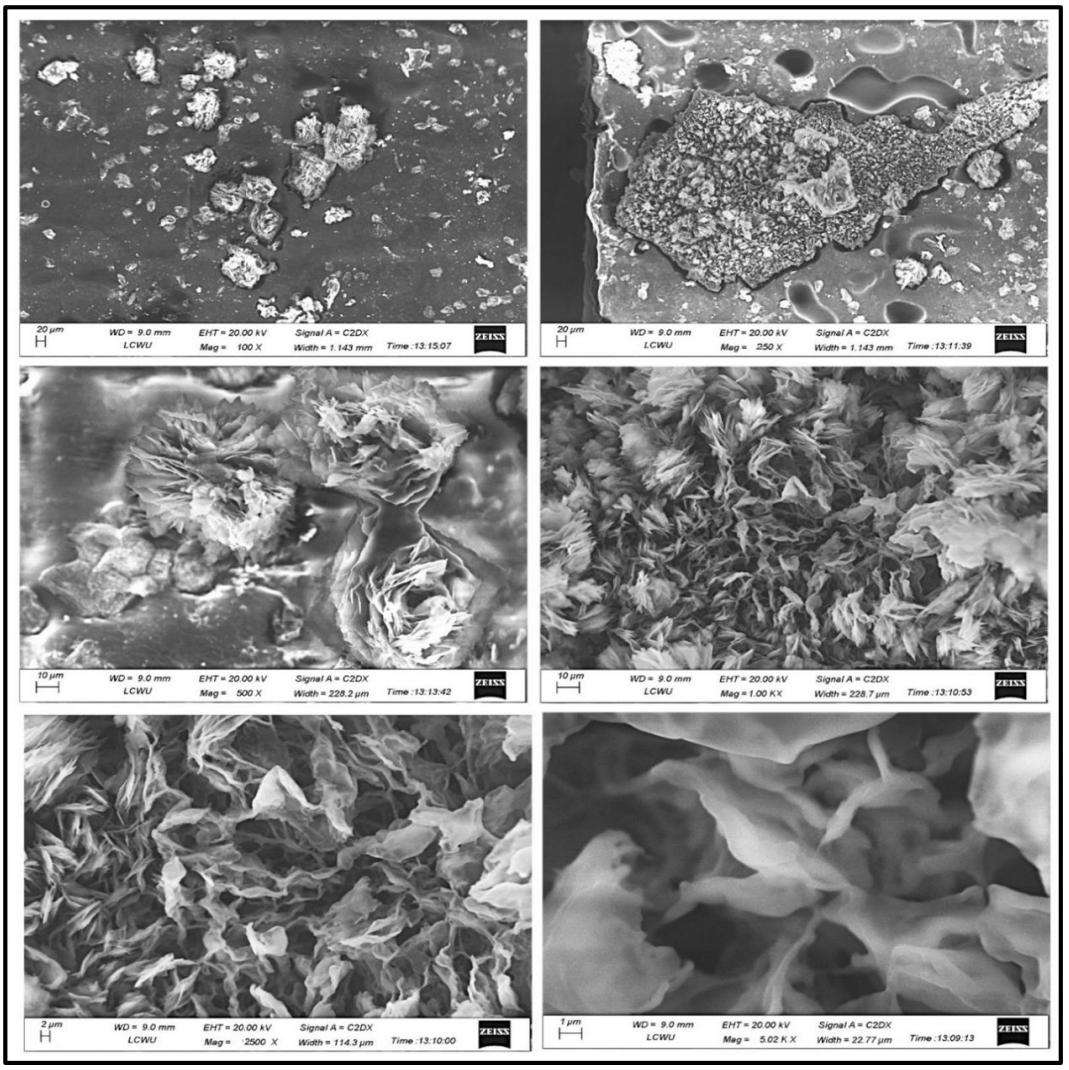

FIGURE 4.4: Scanning electron micrographs of ITZ loaded PCL nanoparticles depicting particle agglomeration at lower magnifications (A, B) and the characteristic porous, flake-like, and rough surface morphology at higher magnifications (C–F), supporting their suit

4.6 FTIR Analysis

FTIR spectroscopy was conducted to evaluate potential physicochemical interactions between Itraconazole (ITZ), polycaprolactone (PCL), Poloxamer 407 (POL), and to confirm the successful incorporation of ITZ into the nanoparticle matrix (Figure 4.5).

The FTIR spectrum of pure ITZ exhibited characteristic absorption bands at approximately 1700 $cm^{-}1$ corresponding to carbonyl (C=O) stretching vibrations, and at 1515 $cm^{-}1$, attributed to C=C stretching within the aromatic rings [107].

The spectrum of PCL displayed a prominent ester carbonyl (C=O) stretching band at 1720 $cm^{-}1$ and methylene ($-CH_2$) stretching vibrations around 2940 $cm^{-}1$, confirming the presence of the aliphatic polyester backbone [108]. Poloxamer 407 demonstrated its typical spectral features, with strong C–O–C stretching vibrations at approximately 1100 $cm^{-}1$ and characteristic C–H stretching bands near 2880 $cm^{-}1$ [109]. The FTIR spectrum of the ITZ-loaded PCL nanoparticle formulation retained all major characteristic peaks of ITZ, PCL, and POL, with minor shifts and peak broadening, particularly in the regions corresponding to C=O and C–O–C stretching vibrations. Notably, no new peaks or significant changes in the spectral profile were observed, indicating the absence of chemical interactions or covalent bond formation between the drug and the excipients [110].

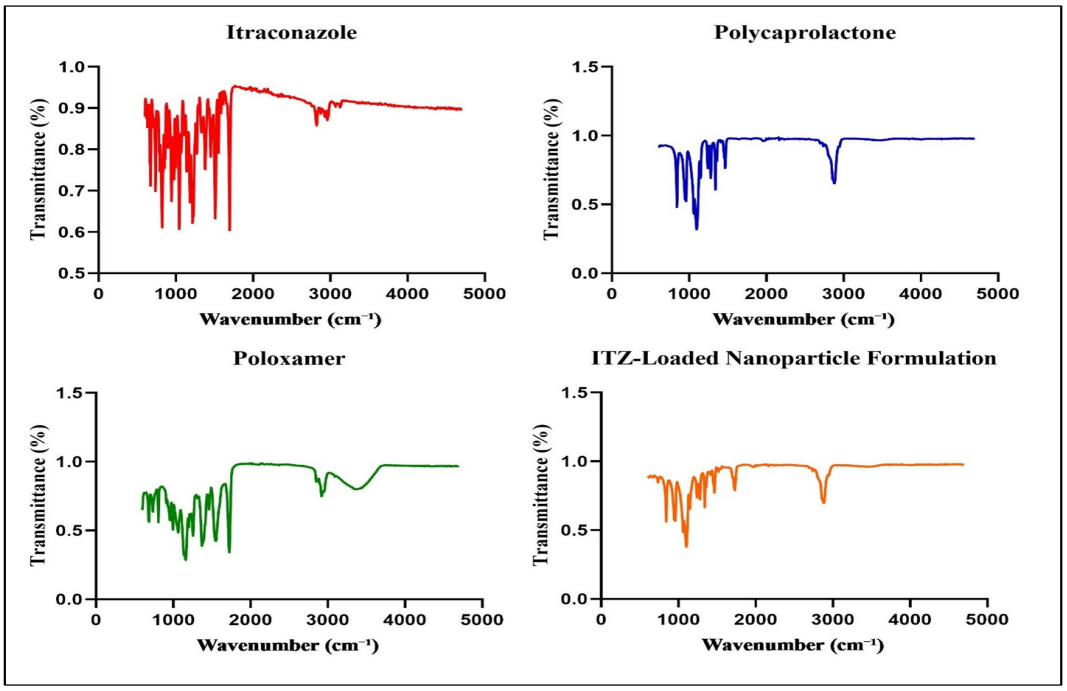

FIGURE 4.5: FTIR spectra of pure Itraconazole (ITZ), polycaprolactone (PCL), Poloxamer 407 (POL), and ITZ-loaded nanoparticle formulation

These findings suggest that ITZ was physically encapsulated within the polymeric matrix without undergoing structural modification. The observed minor shifts and broadening are likely attributable to hydrogen bonding and weak physical interactions between the drug and polymer components, which are commonly reported in nanoparticulate systems [111]. The preservation of key functional groups and the

absence of additional peaks confirm the chemical compatibility of the components and the successful entrapment of ITZ within the nanoparticle system.

4.7 X-Ray Diffraction Pattern

The crystalline behaviour of pure components and the ITZ-loaded nanoparticle formulation was systematically evaluated using X-ray diffraction (XRD), with the diffraction patterns presented in Figure 4.6. Pure ITZ exhibited multiple sharp and intense diffraction peaks at 2θ values of approximately 12.5°, 15.8°, 17.3°, 19.5°, 21.7°, and 25.4°, confirming its highly crystalline nature [112]. These distinct peaks are characteristic of the ordered lattice structure of ITZ. In contrast, PCL displayed a broad, diffused halo centered around 20.2° 2θ, accompanied by a weak crystalline peak at approximately 23.5°, indicative of its semi-crystalline structure. This behaviour reflects the partial crystalline domains typical of PCL-based polymers. Similarly, the Poloxamer diffractogram revealed intense, sharp peaks located at 19.2°, 23.3°, 36.1°, 42.5°, and 62.8°, confirming its crystalline nature, consistent with literature reports for Poloxamer 407. Remarkably, the ITZ-loaded nanoparticle formulation demonstrated a significant loss of the characteristic crystalline peaks of ITZ, exhibiting only a broad, amorphous halo between 15° and 35° 2θ, corresponding to the polymeric matrix.

The complete disappearance of ITZ-specific peaks confirms successful molecular dispersion of the drug within the polymeric carrier system, resulting in amorphization. The absence of crystalline ITZ signals, coupled with the broad amorphous profile of the formulation, suggests effective drug-polymer interactions that inhibit drug recrystallization. This transformation from crystalline to amorphous state is particularly advantageous, as it is well-recognized to enhance drug solubility, dissolution rate, and ultimately, bioavailability [113]. These XRD findings substantiate the successful fabrication of a physically stable, amorphous ITZ-loaded nanoparticle system with promising potential for improving the oral bioavailability of poorly soluble drugs.

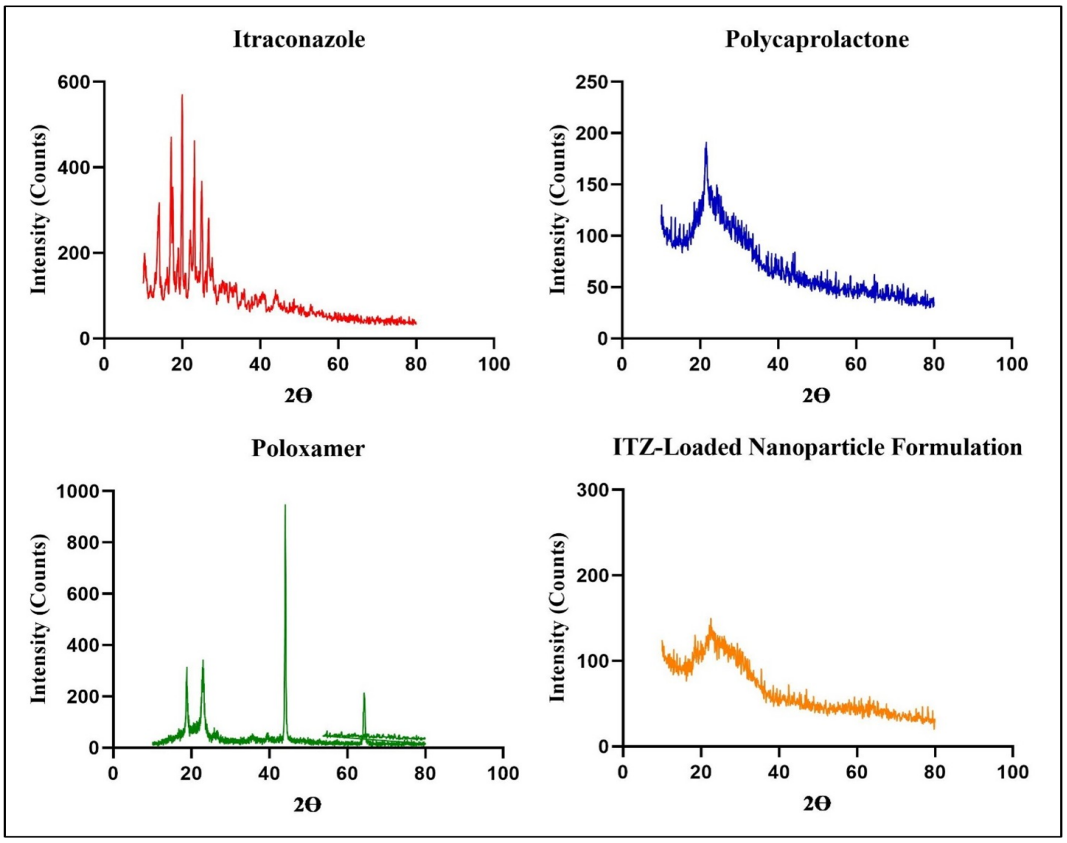

FIGURE 4.6: XRD Patterns of Pure Itraconazole (ITZ), Polycaprolactone (PCL), Poloxamer 407(POL) and ITZ-Loaded Nanoparticle Formulation

4.8 Differential Scanning Calorimetry Analysis

Differential Scanning Calorimetry (DSC) was conducted to evaluate the thermal behaviour and physical state of Itraconazole (ITZ) within the PCL–Poloxamer nanoparticle matrix as shown in Figure 4.7. The thermogram of pure ITZ exhibited a sharp endothermic peak at approximately 166–168°C, corresponding to its melting point, which confirms its crystalline nature [114].

In contrast, this peak value in the thermogram of nanoparticles loaded with ITZ was absent or significantly decreased, suggesting that the drug is converted into an amorphous or molecularly dispersed state within the polymeric system. The PCL showed a melting point of around 59–61°C, which is in line with its semi-crystalline polyester structure, and this peak was maintained in the nanoparticle formulation, although with a reduced intensity, probably due to the plasticizing effect of Poloxamer 407 [115]. Poloxamer showed two distinct endothermic peaks

at 59.09°C and 197.62°C indicating the presence of an ordered crystalline structure. Blank nanoparticle formulation exhibited a broad and less intense thermal transition compared to excipients. The absence of a sharp ITZ peak in the formulation thermogram is a confirmation of successful encapsulation and indicates that the drug is not chemically involved but rather physically incorporated into the PCL matrix. The transition of ITZ from a crystalline to an amorphous state is particularly advantageous for enhancing the solubility and dissolution rate of poorly water-soluble drugs such as ITZ. These findings are consistent with previous reports in which the disappearance or enhancement of ITZ melting peaks in DSC thermogram was attributed as evidence of drug amorphization and uniform dispersion within nanoparticle carriers[113].

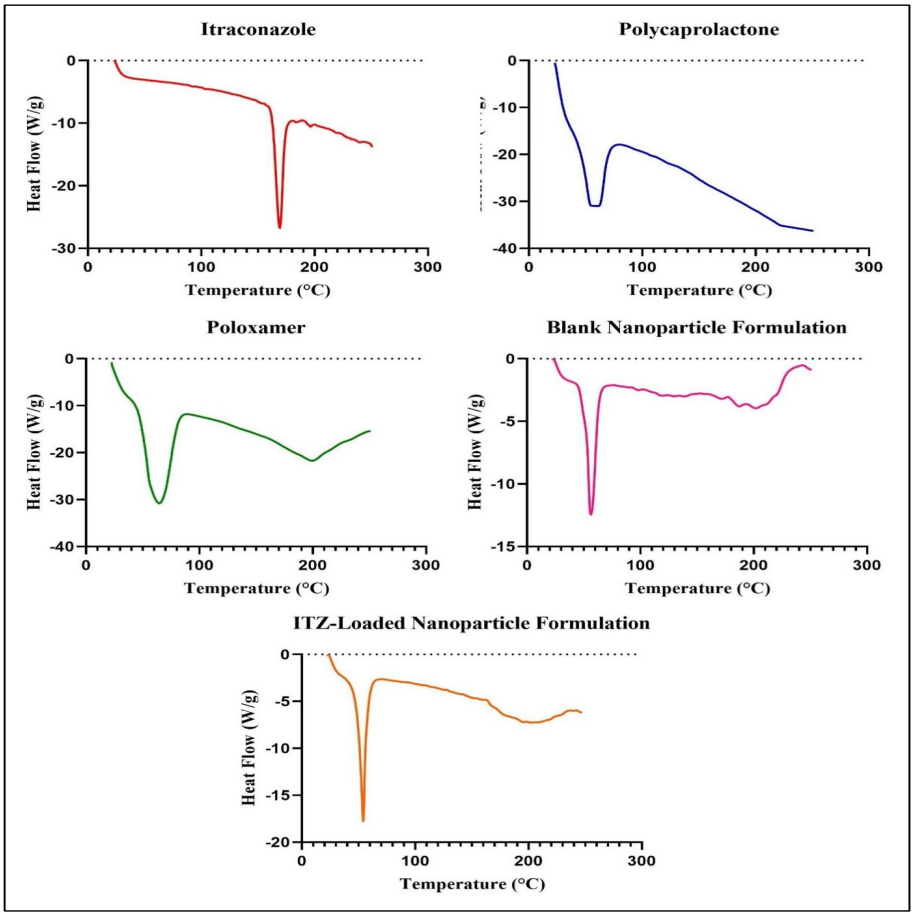

FIGURE 4.7: DSC thermogram of Pure Itraconazole (ITZ), Polycaprolactone (PCL), Poloxamer 407(POL), Blank Nanoparticle Formulation and ITZ-Loaded Nanoparticle Formulation

4.9 Thermo-gravimetric Analysis

Thermo-gravimetric analysis (TGA) was employed to investigate the thermal degradation profiles of pure Itraconazole (ITZ) and ITZ-loaded polycaprolactone (PCL) nanoparticles (Figure. 4.8). The thermogram of pure ITZ revealed a sharp, single-step degradation event initiating at 369.37°C, consistent with its intrinsic decomposition behaviour [116]. The PCL degraded with significant mass losses between 250–350°C due to breakdown of its polymer backbone, whereas Poloxamer started degrading around 150°C, likely because of the breakdown of its PEO-PPO segments. The blank nanoparticle formulation showed a multi-phase degradation pattern comprising loss of moisture below 100°C and polymer decomposition in the range of 200-350°C.

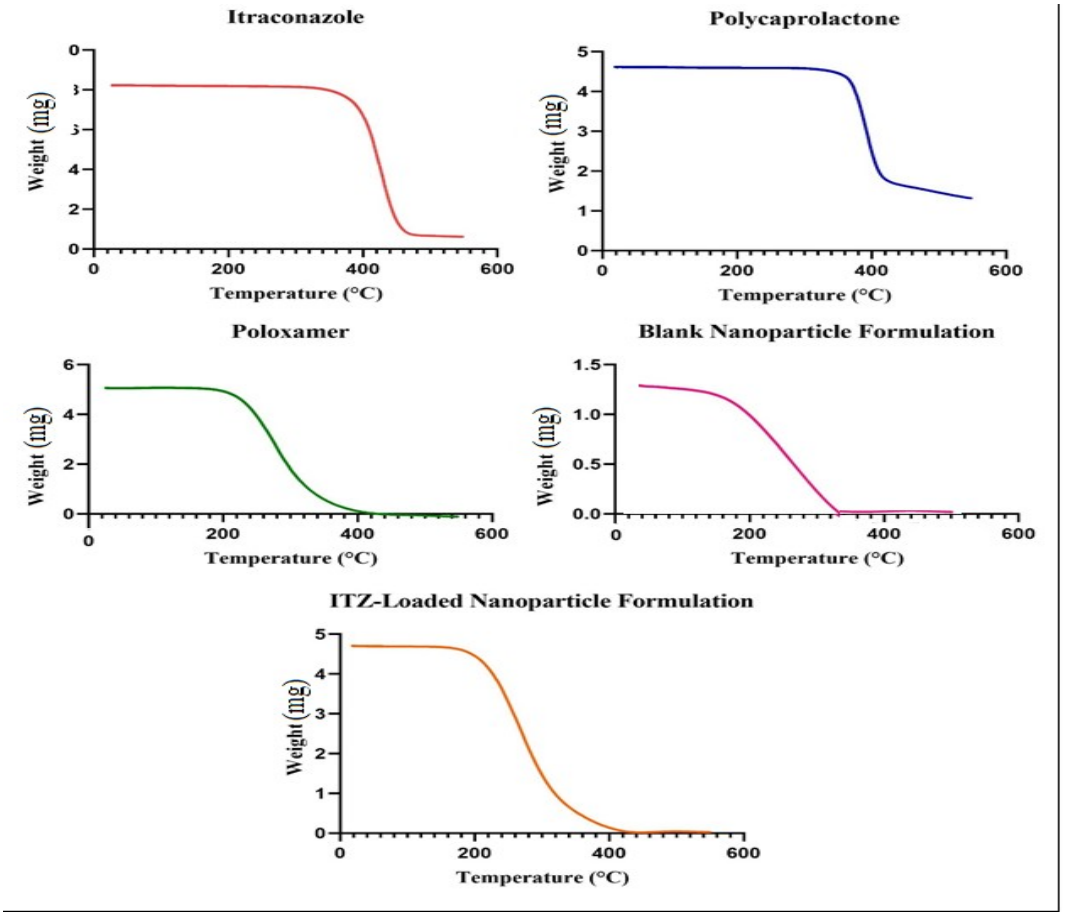

FIGURE 4.8: TGA thermogram of Pure Itraconazole (ITZ), Polycaprolactone (PCL), Poloxamer 407(POL), Blank Nanoparticle Formulation and ITZ-Loaded Nanoparticle Formulation

In contrast, the ITZ-loaded nanoparticle formulation exhibited a multi-phase degradation pattern, characteristic of polymeric drug-delivery systems. The initial weight loss (5–8%) below 100°C was attributed to the evaporation of residual moisture.

The primary degradation occurred between 250–380°C, corresponding to the thermal decomposition of the PCL polymer backbone and the encapsulated ITZ. Crucially, the absence of a distinct ITZ degradation peak at 230°C in the nanoparticle formulation confirmed effective drug encapsulation within the polymeric matrix, with a concomitant shift in degradation onset temperatures. This observation suggests enhanced thermal stabilization of ITZ due to molecular-level dispersion within the PCL nanoparticles, as previously reported [117].

The improved thermal stability of the ITZ-loaded nanoparticles is of significant practical relevance, ensuring compatibility with pharmaceutical processing techniques such as lyophilization and sterilization. These findings underscore the suitability of PCL-based nanoparticles for the delivery of thermolabile drugs like ITZ.

4.10 Physical Evaluation of ITZ-Loaded Nanogel Formulation

The developed nanogel formulation containing ITZ-loaded PCL nanoparticles in a Carbopol 934 matrix has demonstrated promising pharmacological properties that are suitable for topical administration. The findings are summarized in Table 4.3.

The gel was translucent and homogeneous, no observable phase separation or grittiness, indicating effective nanoparticle dispersion and formulation stability. Compatibility with stratum corneum at pH 6.46 $\pm$ 0.01 and minimization of the risk of local irritation make it suitable for topical administration [118] [119]. Rheological analysis revealed pseudoplastic (non-Newtonian) flow behaviour that is beneficial for topical formulations. Furthermore, the spreadability value of 6.08 $\pm$ 0.12 cm indicates sufficient flow characteristics, ensuring effortless application with minimal

mechanical force. Overall, the results confirm the physical resistance, ease of use and suitability of the formulation for effective local administration of Itraconazole.

TABLE 4.3: Physicochemical and Rheological Evaluation of ITZ-Loaded Nanogel

Parameter	**Result (Mean ± SD)**	**Interpretation**
Appearance	Translucent, homogeneous gel	No phase separation or grittiness observed
pH	6.46 ± 0.01	Within physiological range; safe for dermal application
Viscosity (cP at 0.5 rpm)	13,360 ± 125	Suitable for topical use; shear-thinning behaviour
Rheological behaviour	Pseudoplastic (non-Newtonian)	Promote spreadability and retention on skin
Spreadability (cm)	6.08 ± 0.12	Ensures ease of application with minimal mechanical force

4.11 Ex Vivo Skin Permeation Study

Ex vivo skin permeation studies revealed a significantly enhanced transdermal delivery of Itraconazole (ITZ) from the F2 nanoparticle-loaded gel compared to the plain ITZ gel. After 24 hours, the cumulative drug permeation (Q) from the F2 nanoparticle gel reached 173.29±3.12μg/cm^2, representing a 129.9% increase relative to the plain gel (75.35±1.35μg/cm^2) ($p<0.001$), as illustrated in Figure 4.9. This remarkable improvement can be attributed to the nanometric particle size of the formulation, which enhances surface area and facilitates deeper penetration into the skin layers. Furthermore, the incorporation of Poloxamer 407, a well-established permeation enhancer, likely contributed to this effect by disrupting intercellular lipid bilayers and increasing skin hydration, thereby promoting drug

transport across the stratum corneum [120] [121]. The steady-state flux (Jss) of the F2 nanoparticle gel was also significantly higher (6.32±0.15μg/cm^2/h) compared to the plain gel (2.58±0.08μg/cm^2/h), corresponding to a 145% increase ($p<0.001$), further confirming the superior permeation profile of the nanoparticle-based system (Table 4.4).

Additionally, the calculated Enhancement Ratio (ER) for the F2 nanoparticle gel was 2.45, indicating a more than two-fold enhancement in permeation compared to the plain gel. As ER is a derived parameter based on Jss, no statistical comparison was performed for this value.

These findings are consistent with previous reports demonstrating that nanocarrier-based formulations can significantly improve the transdermal delivery of poorly water-soluble, lipophilic antifungal agents [63] [66].

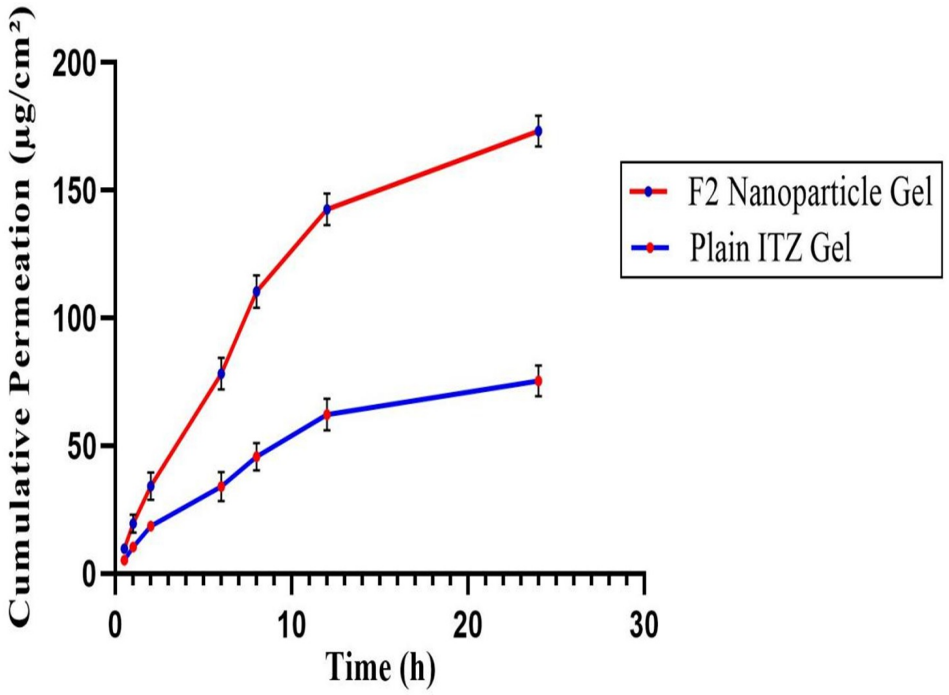

FIGURE 4.9: Cumulative permeation of ITZ from Plain ITZ Gel and F2 Nanoparticle Gel across excised rabbit skin (Mean±SD, n=3)

TABLE 4.4: Permeation parameters of ITZ from plain gel and F2 nanogel (Mean ± SD, n = 3)

Parameter	**Plain ITZ Gel**	**F2 Nanoparticle Gel**	**p-value**	**Sig.**
Q24 ($\mu g/cm^2$)	75.35±1.35	173.29±3.12	<0.001	***
Jss ($\mu g/cm^2/h$)	2.58±0.08	6.32±0.15	<0.001	***
Enhancement Ratio (ER)	1 (Reference)	2.45		

4.12 Skin Irritation Test

The skin irritation potential of the nanogel incorporating ITZ-loaded polycaprolactone (PCL) nanoparticles was evaluated using the Draize dermal irritation test in New Zealand White rabbits (n = 9), distributed into three groups: test (n = 3), positive control (0.8% sodium lauryl sulfate), and negative control (untreated). As shown in Figure 4.10 and Table 4.5, only mild erythema (score 1) occurred in two of the three test animals 24 hours after application, and it completely disappeared within 48 hours. No oedema or behavioural signs of irritation (e.g., scratching or discomfort) were observed at any time point. The mean primary irritation index (PII) in the test group was 0.33 ± 0.58, which classified the product as non-irritating according to OECD criteria (PII < 1.0) [122][123].

In contrast, the positive control group (0.8 % sodium lauryl sulphate) showed significant erythema (score 2-3) and mild oedema at 24 hours, which resolved in all animals only partially at 72 hours. The negative control group (untreated sites) remained completely free of erythema or swelling at all time points, confirming the integrity of the skin and no spontaneous irritation. The favorable dermal safety profile of the nanogel is attributed to the biocompatibility of the PCL nanoparticles, which are well-established biodegradable polymers with low

toxicity and immunogenicity, and to the presence of eucalyptus oil, which may have protective properties. Eucalyptus oil is known to reduce dermal inflammation and histamine-induced oedema by modulating vascular permeability and the release of inflammatory mediators [124].

In addition, visual inspection of the application points (Figure 4.10) these findings were supported by the fact that the skin of the test group was intact, without visible lesions, peeling or redness after 24 hours.

These results confirm the suitability of the nanogel loaded with ITZ for topical application and ensure both therapeutic efficacy and skin safety.

*PII (Test Group) = 0.00 → Classified as Non-Irritant

*PII (Positive Control) = 3.00 → Classified as Severe Irritant

* PII (Negative Control) = 0.00 → No irritation observed

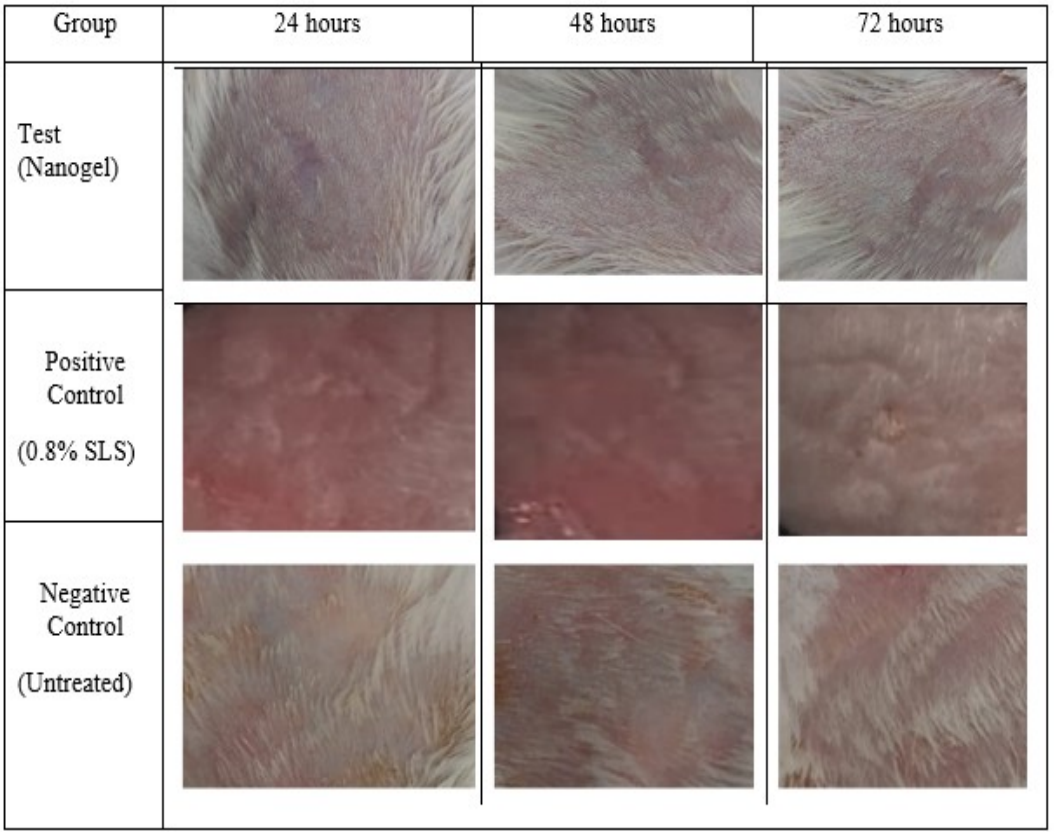

FIGURE 4.10: Comparison of Skin Irritation Responses Over 24, 48 and 72 Hours across Test Group, Positive Control, and Negative Control Groups

Table 4.5: Skin Irritation Scores at 24 h, 48 h and 72 h in New Zealand White Rabbits

		(24 hour)			**(48 Hour)**			**(72 hour)**		
Group	**Animal**	**Erythema**	**Edema**	**Total**	**Erythema**	**Edema**	**Total**	**Erythema**	**Edema**	**Total**
	1	0	0	0	0	0	0	0	0	0
Test (Nanogel)	2	0	0	0	0	0	0	0	0	0
	3	0	0	0	0	0	0	0	0	0
Mean ± SD		0 ±0.00	0±0.00	0±0.00	0 ±0.00	0±0.00	0±0.00	0±0.00	0±0.00	0±0.00
Positive Control	4	2	1	3	2	1	3	2	1	3
	5	3	1	4	2	1	3	2	1	3
(0.8% SLS)	6	3	2	5	2	1	3	2	1	3
Mean ±SD		2.67 ±0.58	1.33 ±0.58	4.00 ±1.00	2.00±0.00	1.00 ±0.00	3.00 ±0.00	2.00±0.20	1.00 ±0.00	3.00 ±0.00
Negative Control	7	0	0	0	0	0	0	0	0	0
	8	0	0	0	0	0	0	0	0	0
(Untreated)	9	0	0	0	0	0	0	0	0	0
Mean ± SD		0 ± 0.00	0±0.00	0±0.00	0±0.00	0±0.00	0±0.00	0±0.00	0±0.00	0±0.00

4.13 Stability

Stability tests were performed to assess the physical integrity, pH consistency and rheological behaviour of the F2 gel formulation for three months under the storage conditions recommended in the ICH Q1A(R^2) guidelines.

The powder was stored under three temperature conditions: refrigerated (4 ± 1°C), ambient (25 ± 2°C), and accelerated (40 ± 2°C / 75 ± 5% RH) as indicated in Table 4.6.

The optimized F2 formulation was evaluated at 1, 2, and 3 months for visual characteristics, pH, and viscosity. The optimized F2 formulation was physically stable throughout the study.

No changes in appearance, such as phase separation, precipitation or coloring, were observed under any of the test conditions, which confirmed the physical integrity of the formulation. The initial pH of F2 was 6.48 ± 0.02.

The pH ranged within the acceptable range of ±0.5 units in all storage conditions and time points. In accelerated conditions (40°C), a slight decrease in pH was observed, reaching 6.22 ± 0.03 over three months, but still within the stability limits.

The change in viscosity at refrigerated and ambient temperatures was <5%. At 40°C, the viscosity decreased gradually, with a maximum decrease of approximately 7.95% after three months. These changes remained within the pre-specified margin of error of ±10%.

Moreover, the formulation retained its shear-thinning behaviour, which indicates structural integrity of the gel matrix.

The decrease in viscosity at higher temperatures is attributable to the relaxation of the polymer or to the decreased hydrogen bonding interactions due to thermal stress [125] [126]. However, the F2 formulation has maintained its rheological and physicochemical properties, which supports its suitability for long-term storage.

Table 4.6: Stability parameters of F2 Gel Formulation stored under ICH conditions over 3 months

Time (months)	Storage Temp	Appearance	pH ± SD	Viscosity (cP) ± SD	% Viscosity Change
1	4°C	Clear, homogeneous	6.46 ± 0.01	13360 ± 125	-0.67%
1	25°C	Clear, homogeneous	6.43 ± 0.02	13220 ± 150	-1.71%
1	40°C	Clear, homogeneous	6.38 ± 0.03	12890 ± 170	-4.16%
2	4°C	Clear, homogeneous	6.44 ± 0.02	13290 ± 120	-1.19%
2	25°C	Clear, homogeneous	6.39 ± 0.02	13150 ± 135	-2.23%
2	40°C	Clear, homogeneous	6.29 ± 0.04	12650 ± 160	-5.95%
3	4°C	Clear, homogeneous	6.42 ± 0.02	13190 ± 110	-1.93%
3	25°C	Clear, homogeneous	6.34 ± 0.03	12970 ± 145	-3.56%
3	40°C	Clear, homogeneous	6.22 ± 0.03	12380 ± 130	-7.95%

Chapter 5

Conclusion and Future Recommendations

5.1 Conclusion

This study successfully developed pH-responsive PCL nanoparticles for enhanced transdermal delivery of ITZ. The optimized F2 formulation exhibited superior characteristics, including high encapsulation efficiency (88.4±1.2%), uniform particle size (154.6nm), and excellent colloidal stability (zeta potential: 10.7±5.36mV). The nanoparticles demonstrated pH-dependent drug release, achieving 80.41% and 94.34% cumulative release at pH 5.5 (skin pH) and pH 7.4 (physiological pH), respectively, following Higuchi kinetics (R^2=0.9804 at pH 5.5), indicative of a diffusion-controlled release mechanism. Comprehensive physicochemical analyses (FTIR, XRD, DSC, TGA, and SEM) confirmed the amorphous state of ITZ within the polymeric matrix and the absence of drug–polymer interactions, ensuring formulation stability and drug efficacy. Ex vivo permeation studies revealed a 2.45-fold increase in steady-state flux (Jss=6.32±0.15μg/cm^2/h) compared to plain ITZ gel, attributed to the nanometric particle size and the permeation-enhancing properties of Poloxamer 407. The nanogel formulation exhibited favorable rheological properties (viscosity: 13,360±125cP; spreadability: 6.08±0.12cm) and remained

stable for three months under ICH-recommended storage conditions. Skin irritation studies (Draize test) confirmed excellent biocompatibility (PII = 0), with no signs of erythema or edema.

Overall, these findings highlight the potential of PCL-based nanoparticles as a versatile and biocompatible platform for transdermal delivery of poorly soluble antifungal agents like ITZ, offering sustained release, enhanced permeation, and improved therapeutic outcomes. This approach addresses the limitations of conventional formulations and provides a promising strategy for targeted antifungal therapy.

5.2 Future Recommendations

The findings of this study open numerous avenues for further research and development in the field of nanogel-based antifungal drug delivery. The following key recommendations are proposed:

Firstly, it is recommended that more extensive in vivo studies be conducted to evaluate the pharmacokinetics, biodistribution, and therapeutic efficacy of polycaprolactone based nanogels containing Itraconazole. While in vitro findings suggest enhanced skin permeation and drug retention, in vivo validation across diverse animal models and eventual human trials is essential to determine safety, efficacy, and systemic absorption levels...

Secondly, future research should explore long-term toxicity and skin irritation profiles associated with repeated application of nanogels, especially in sensitive skin populations and pediatric or geriatric groups. Although PCL, Poloxamer 407, and Carbopol 934 are biocompatible polymers. Thirdly, there is a need to develop scalable and reproducible manufacturing processes for nanogel systems to ensure batch-to-batch consistency. Regulatory frameworks necessitate stringent quality control and assurance mechanisms, and future work must establish scalable protocols that meet GMP (Good Manufacturing Practices) standards. Furthermore,

stability studies under ICH guidelines (climatic zone-specific) should be performed to assess the physicochemical robustness of formulations during storage and transport. Additionally, patient-centric aspects such as cosmetic acceptability, odor, spreadability, residue formation, and ease of application should be prioritized in formulation refinement. From a formulation science perspective, future studies could explore the coencapsulation of multiple antifungal agents or adjunct compounds that may exert synergistic effects, reduce resistance development, and improve broad-spectrum efficacy. In addition to therapeutic improvements, the environmental and economic sustainability of nanogel production should be evaluated. Green synthesis methods, biodegradable solvent systems, and cost-effective materials can enhance accessibility and reduce environmental burden. These efforts are especially relevant for low-resource settings where fungal infections are prevalent but advanced therapies are inaccessible. Lastly, comparative studies with existing commercial formulations should be undertaken to benchmark the developed nanogel system against currently marketed products in terms of efficacy, safety, patient compliance, and cost-effectiveness. These studies should be comprehensive, covering pharmacoeconomics, patient satisfaction, dermatological outcomes, and healthcare resource utilization. Clinical trials with diverse populations and dermatological conditions will be key to successful translation. In conclusion, while this research marks a significant step toward developing a more effective transdermal delivery system for Itraconazole, continuous efforts in translational research, regulatory compliance, sustainable production, and patient-oriented design are crucial to maximize the clinical and commercial impact of such nanogel platforms. Future development should focus on integrated, holistic strategies that address scientific, practical, and socioeconomic dimensions of antifungal therapy.

Ethical Approval Statement

This study received ethical approval from the Research Ethics Committee of the Faculty of Pharmacy, Capital University of Science and Technology, Islamabad (Approval No. REC/FoP/F2024/11). All experimental procedures were conducted in accordance with institutional ethical guidelines

Bibliography

[1] G. Brown *et al.*, "Hidden killers: human fungal infections," *Science Translational Medicine*, vol. 4, no. 165, pp. 165rv13–165rv13, 2012.

[2] B. Havlickova, V. A. Czaika, and M. Friedrich, "Epidemiological trends in skin mycoses worldwide," *Mycoses*, vol. 51, pp. 2–15, 2008.

[3] A. Chowdhary, C. Sharma, and J. F. Meis, "Candida auris: a rapidly emerging cause of hospital-acquired multidrug-resistant fungal infections globally," *PLOS Pathogens*, vol. 13, no. 5, p. e1006290, 2017.

[4] L. Sherry *et al.*, "Biofilm-forming capability of highly virulent, multidrug-resistant candida auris," *Emerging Infectious Diseases*, vol. 23, no. 2, p. 328, 2017.

[5] B. M. Peters, M. E. Shirtliff, and M. A. Jabra-Rizk, "Antimicrobial peptides: primeval molecules or future drugs?," *PLOS Pathogens*, vol. 6, no. 10, p. e1001067, 2010.

[6] M. C. Fisher *et al.*, "Worldwide emergence of resistance to antifungal drugs challenges human health and food security," *Science*, vol. 360, no. 6390, pp. 739–742, 2018.

[7] F. C. Odds, A. J. Brown, and N. A. Gow, "Antifungal agents: mechanisms of action," *Trends in Microbiology*, vol. 11, no. 6, pp. 272–279, 2003.

[8] T. Loftsson and M. E. Brewster, "Pharmaceutical applications of cyclodextrins: basic science and product development," *Journal of Pharmacy and Pharmacology*, vol. 62, no. 11, pp. 1607–1621, 2010.

[9] J. R. Perfect, "The antifungal pipeline: a reality check," *Nature Reviews Drug Discovery*, vol. 16, no. 9, pp. 603–616, 2017.

[10] D. Rosenblum *et al.*, "Progress and challenges towards targeted delivery of cancer therapeutics," *Nature Communications*, vol. 9, no. 1, p. 1410, 2018.

[11] T. W. Prow *et al.*, "Nanoparticles and microparticles for skin drug delivery," *Advanced Drug Delivery Reviews*, vol. 63, no. 6, pp. 470–491, 2011.

[12] A. Lohani *et al.*, "Nanotechnology-based cosmeceuticals," *International Scholarly Research Notices*, vol. 2014, p. 843687, 2014.

[13] T. K. Dash and V. B. Konkimalla, "Poly--caprolactone based formulations for drug delivery and tissue engineering: A review," *Journal of Controlled Release*, vol. 158, no. 1, pp. 15–33, 2012.

[14] R. Rautemaa-Richardson and M. D. Richardson, "Systemic fungal infections," *Medicine*, vol. 45, no. 12, pp. 757–762, 2017.

[15] H. Almeida *et al.*, "Applications of poloxamers in ophthalmic pharmaceutical formulations: an overview," *Expert Opinion on Drug Delivery*, vol. 10, no. 9, pp. 1223–1237, 2013.

[16] S. Pund, G. Rasve, and G. Borade, "Ex vivo permeation characteristics of venlafaxine through sheep nasal mucosa," *European Journal of Pharmaceutical Sciences*, vol. 48, no. 1-2, pp. 195–201, 2013.

[17] M. C. Arendrup and T. F. Patterson, "Multidrug-resistant candida: epidemiology, molecular mechanisms, and treatment," *The Journal of Infectious Diseases*, vol. 216, no. suppl_3, pp. S445–S451, 2017.

[18] J. N. Pawar *et al.*, "Recent development and achievements in solubility and dissolution enhancement of itraconazole: A review," *International Journal of Pharmaceutical Sciences and Research*, vol. 5, no. 8, p. 3096, 2014.

[19] K. Venkatakrishnan, L. L. Von Moltke, and D. J. Greenblatt, "Effects of the antifungal agents on oxidative drug metabolism: clinical relevance," *Clinical Pharmacokinetics*, vol. 38, no. 2, pp. 111–180, 2000.

[20] R. Salama *et al.*, "Recent advances in controlled release pulmonary therapy," *Current Drug Delivery*, vol. 6, no. 4, pp. 404–414, 2009.

[21] G. Tiwari *et al.*, "Drug delivery systems: An updated review," *International Journal of Pharmaceutical Investigation*, vol. 2, no. 1, p. 2, 2012.

[22] K. Pawar *et al.*, "Recent trends in antifungal agents: A reference to formulation, characterization and applications," *Drug Delivery Letters*, vol. 9, no. 3, pp. 199–210, 2019.

[23] A. Balde *et al.*, "Chitosan and its derivatives for nanomaterial formulations: fabrication and physicochemical characterization," in *Chitosan-Based Hybrid Nanomaterials*, pp. 73–89, Elsevier, 2024.

[24] M. Sharma, R. Sharma, and D. Jain, "Nanotechnology based approaches for enhancing oral bioavailability of poorly water soluble antihypertensive drugs," *Scientifica*, vol. 2016, no. 1, p. 8525679, 2016.

[25] J. Lestner and W. Hope, "Itraconazole: an update on pharmacology and clinical use for treatment of invasive and allergic fungal infections," *Expert Opinion on Drug Metabolism & Toxicology*, vol. 9, no. 7, pp. 911–926, 2013.

[26] L. Subedi *et al.*, "Preparation of topical itraconazole with enhanced skin/-nail permeability and in vivo antifungal efficacy against superficial mycosis," *Pharmaceutics*, vol. 13, no. 5, 2021.

[27] N. Isoherranen *et al.*, "Role of itraconazole metabolites in cyp3a4 inhibition," *Drug Metabolism and Disposition*, vol. 32, no. 10, pp. 1121–1131, 2004.

[28] H. Ashbee *et al.*, "Therapeutic drug monitoring (tdm) of antifungal agents: guidelines from the british society for medical mycology," *Journal of Antimicrobial Chemotherapy*, vol. 69, no. 5, pp. 1162–1176, 2014.

[29] T. Hardin *et al.*, "Pharmacokinetics of itraconazole following oral administration to normal volunteers," *Antimicrobial Agents and Chemotherapy*, vol. 32, no. 9, pp. 1310–1313, 1988.

[30] M. Hoenigl and A. F. Talento, "Fungal infections complicating covid-19," *MDPI*, 2021.

[31] A. Amit and R. Rajendra, "Formulation and evaluation of solid lipid-based nano formulation of itraconazole," 2023.

[32] J. Pardeike, A. Hommoss, and R. H. Müller, "Lipid nanoparticles (sln, nlc) in cosmetic and pharmaceutical dermal products," *International Journal of Pharmaceutics*, vol. 366, no. 1-2, pp. 170–184, 2009.

[33] R. Vecchione *et al.*, *Microencapsulation for Biomedical Applications*. Frontiers Media SA, 2022.

[34] L. Gao *et al.*, "Application of drug nanocrystal technologies on oral drug delivery of poorly soluble drugs," *Pharmaceutical Research*, vol. 30, no. 2, pp. 307–324, 2013.

[35] C. Tapeinos, M. Battaglini, and G. Ciofani, "Advances in the design of solid lipid nanoparticles and nanostructured lipid carriers for targeting brain diseases," *Journal of Controlled Release*, vol. 264, pp. 306–332, 2017.

[36] J. Zhang *et al.*, "Ten years of knowledge of nano-carrier based drug delivery systems in ophthalmology: current evidence, challenges, and future prospective," *International Journal of Nanomedicine*, pp. 6497–6530, 2021.

[37] H. Makadia and S. Siegel, "Poly lactic-co-glycolic acid (plga) as biodegradable controlled drug delivery carrier," *Polymers*, vol. 3, no. 3, pp. 1377–1397, 2011.

[38] E. Bseiso *et al.*, "Recent advances in topical formulation carriers of antifungal agents," *Indian Journal of Dermatology, Venereology and Leprology*, vol. 81, p. 457, 2015.

[39] F. Danhier *et al.*, "Plga-based nanoparticles: an overview of biomedical applications," *Journal of Controlled Release*, vol. 161, no. 2, pp. 505–522, 2012.

[40] T. Ways, W. Lau, and V. Khutoryanskiy, "Chitosan and its derivatives for application in mucoadhesive drug delivery systems," *Polymers*, vol. 10, no. 3, p. 267, 2018.

[41] L. Moura *et al.*, "Recent advances on the development of wound dressings for diabetic foot ulcer treatment—a review," *Acta Biomaterialia*, vol. 9, no. 7, pp. 7093–7114, 2013.

[42] N. Ubrich *et al.*, "Preparation and characterization of propranolol hydrochloride nanoparticles: a comparative study," *Journal of Controlled Release*, vol. 97, no. 2, pp. 291–300, 2004.

[43] G. Dumortier *et al.*, "A review of poloxamer 407 pharmaceutical and pharmacological characteristics," *Pharmaceutical Research*, vol. 23, no. 12, pp. 2709–2728, 2006.

[44] H. Almeida *et al.*, "Pluronic® f127 and pluronic lecithin organogel (plo): Main features and their applications in topical and transdermal administration of drugs," *Journal of Pharmacy & Pharmaceutical Sciences*, vol. 15, no. 4, pp. 592–605, 2012.

[45] E. Ruel-Gariépy and J.-C. Leroux, "In situ-forming hydrogels—review of temperature-sensitive systems," *European Journal of Pharmaceutics and Biopharmaceutics*, vol. 58, no. 2, pp. 409–426, 2004.

[46] K. Al Khateb *et al.*, "In situ gelling systems based on pluronic f127/pluronic f68 formulations for ocular drug delivery," *International Journal of Pharmaceutics*, vol. 502, no. 1-2, pp. 70–79, 2016.

[47] R. Khullar *et al.*, "Formulation and evaluation of mefenamic acid emulgel for topical delivery," *Saudi Pharmaceutical Journal*, vol. 20, no. 1, pp. 63–67, 2012.

[48] N. Peppas *et al.*, "Hydrogels in pharmaceutical formulations," *European Journal of Pharmaceutics and Biopharmaceutics*, vol. 50, no. 1, pp. 27–46, 2000.

[49] B. Bash and K. Prakasam, "Formulation and evaluations of gel containing fluconazole-antifungal agent," 2011.

[50] Y. Zheng *et al.*, "Effects of carbopol® 934 proportion on nanoemulsion gel for topical and transdermal drug delivery: A skin permeation study," *International Journal of Nanomedicine*, pp. 5971–5987, 2016.

[51] N. Hamdi *et al.*, "An insight into the use and advantages of carbopol in topical mucoadhesive drug delivery system: A systematic review," *Journal of Pharmacy*, vol. 3, no. 1, pp. 53–65, 2023.

[52] N. Nafee *et al.*, "Design and characterization of mucoadhesive buccal patches containing cetylpyridinium chloride," *Acta Pharmaceutica (Zagreb, Croatia)*, vol. 53, no. 3, pp. 199–212, 2003.

[53] Y. Zhou *et al.*, "Crossing the blood-brain barrier with nanoparticles," *Journal of Controlled Release*, vol. 270, pp. 290–303, 2018.

[54] M. Madan *et al.*, "In situ forming polymeric drug delivery systems," *Indian Journal of Pharmaceutical Sciences*, vol. 71, no. 3, p. 242, 2009.

[55] M. Nakarani *et al.*, "Itraconazole nanosuspension for oral delivery: Formulation, characterization and in vitro comparison with marketed formulation," *Daru: Journal of Faculty of Pharmacy, Tehran University of Medical Sciences*, vol. 18, no. 2, p. 84, 2010.

[56] V. Mishra *et al.*, "Solid lipid nanoparticles: Emerging colloidal nano drug delivery systems," *Pharmaceutics*, vol. 10, no. 4, p. 191, 2018.

[57] M. Rizwan *et al.*, "Enhanced transdermal drug delivery techniques: an extensive review of patents," *Recent Patents on Drug Delivery & Formulation*, vol. 3, no. 2, pp. 105–124, 2009.

[58] B. Gajra, C. Dalwadi, and R. Patel, "Formulation and optimization of itraconazole polymeric lipid hybrid nanoparticles (lipomer) using box behnken design," *DARU Journal of Pharmaceutical Sciences*, vol. 23, no. 1, p. 3, 2015.

[59] T. B. Patel, T. R. Patel, and B. Suhagia, "Preparation, characterization, and optimization of microemulsion for topical delivery of itraconazole," *Journal of Drug Delivery & Therapeutics*, vol. 8, no. 2, pp. 136–145, 2018.

[60] C. Yang *et al.*, "Recent advances in the application of vitamin e tpgs for drug delivery," *Theranostics*, vol. 8, no. 2, p. 464, 2018.

[61] N. Kumar and S. Goindi, "Development and optimization of itraconazole-loaded solid lipid nanoparticles for topical administration using high shear homogenization process by design of experiments: in vitro, ex vivo and in vivo evaluation," *AAPS PharmSciTech*, vol. 22, no. 7, p. 248, 2021.

[62] E.-S. Ha *et al.*, "Application of diethylene glycol monoethyl ether in solubilization of poorly water-soluble drugs," *Journal of Pharmaceutical Investigation*, vol. 50, pp. 231–250, 2020.

[63] P. Kesharwani *et al.*, "Itraconazole and difluorinated-curcumin containing chitosan nanoparticle loaded hydrogel for amelioration of onychomycosis," *Biomimetics*, vol. 7, no. 4, p. 206, 2022.

[64] S. Mehrandish, G. Mohammadi, and S. Mirzaeei, "Preparation and functional evaluation of electrospun polymeric nanofibers as a new system for sustained topical ocular delivery of itraconazole," *Pharmaceutical Development and Technology*, vol. 27, no. 1, pp. 25–39, 2022.

[65] A. Patil *et al.*, "Formulation and evaluation of itraconazole-loaded nanoemulgel for efficient topical delivery to treat fungal infections," *Therapeutic Delivery*, vol. 15, no. 3, pp. 165–179, 2024.

[66] J. Passos *et al.*, "Development, skin targeting and antifungal efficacy of topical lipid nanoparticles containing itraconazole," *European Journal of Pharmaceutical Sciences*, vol. 149, p. 105296, 2020.

[67] A. Anselmo and S. Mitragotri, "An overview of clinical and commercial impact of drug delivery systems," *Journal of Controlled Release*, vol. 190, pp. 15–28, 2014.

[68] S. Mukherjee, S. Ray, and R. Thakur, "Solid lipid nanoparticles: a modern formulation approach in drug delivery system," *Indian Journal of Pharmaceutical Sciences*, vol. 71, no. 4, p. 349, 2009.

[69] R. Barreiro-Iglesias, C. Alvarez-Lorenzo, and A. Concheiro, "Incorporation of small quantities of surfactants as a way to improve the rheological and diffusional behaviour of carbopol gels," *Journal of Controlled Release*, vol. 77, no. 1-2, pp. 59–75, 2001.

[70] M. Saqib *et al.*, "Amphotericin b loaded polymeric nanoparticles for treatment of leishmania infections," *Nanomaterials*, vol. 10, no. 6, p. 1152, 2020.

[71] J. Abriata *et al.*, "Development, characterization and biological in vitro assays of paclitaxel-loaded pcl polymeric nanoparticles," *Materials Science and Engineering: C*, vol. 96, pp. 347–355, 2019.

[72] A. Stancu *et al.*, "Development, optimization, and evaluation of new gel formulations with cyclodextrin complexes and volatile oils with antimicrobial activity," *Gels*, vol. 10, no. 10, p. 645, 2024.

[73] T. Soundarya *et al.*, "A novel one-pot synthesis strategy for -mnvo nanorods synthesized via 1-(3,6-dioxaheptane) 3-methyl imidazolium methane sulfonate-assisted hydrothermal route for sustainable and on-demand advanced supercapacitor electrodes and as negative electrode materials for li-ion batteries," *Journal of Energy Storage*, vol. 85, p. 111076, 2024.

[74] R. Yadollahi, K. Vasilev, and S. Simovic, "Nanosuspension technologies for delivery of poorly soluble drugs," *Journal of Nanomaterials*, vol. 2015, no. 1, p. 216375, 2015.

[75] H. Hamishehkar *et al.*, "Evaluation of solubility and dissolution profile of itraconazole after cogrinding with various hydrophilic carriers," *Journal of Drug Delivery Science and Technology*, vol. 24, no. 6, pp. 653–658, 2014.

[76] S. Botros, A. Hussein, and H. Mansour, "A novel nanoemulsion intermediate gel as a promising approach for delivery of itraconazole: design, in vitro and ex vivo appraisal," *AAPS PharmSciTech*, vol. 21, pp. 1–13, 2020.

[77] N. Damodharan, "Mathematical modelling of dissolution kinetics in dosage forms," *Research Journal of Pharmacy and Technology*, vol. 13, no. 3, pp. 1339–1345, 2020.

[78] E. Ertugral-Samgar, A. Ozmen, and O. Gok, "Thermo-responsive hydrogels encapsulating targeted core–shell nanoparticles as injectable drug delivery systems," *Pharmaceutics*, vol. 15, no. 9, p. 2358, 2023.

[79] H. Danafar *et al.*, "Biodegradable m-peg/pcl core-shell micelles: preparation and characterization as a sustained release formulation for curcumin," *Advanced Pharmaceutical Bulletin*, vol. 4, no. Suppl 2, p. 501, 2014.

[80] S. El-Housiny *et al.*, "Fluconazole-loaded solid lipid nanoparticles topical gel for treatment of pityriasis versicolor: formulation and clinical study," *Drug Delivery*, vol. 25, no. 1, pp. 78–90, 2018.

[81] H. Ho *et al.*, "Development of itraconazole-loaded polymeric nanoparticle dermal gel for enhanced antifungal efficacy," *Journal of Nanomaterials*, vol. 2020, no. 1, p. 8894541, 2020.

[82] B. Hazer *et al.*, "Free radical polymerization of dimethyl amino ethyl methacrylate initiated by poly (3-hydroxybutyrate-co-3-hydroxyhexanoate) macroazo initiator: Thermal and physicochemical characterization," *Journal of Polymers and the Environment*, vol. 31, no. 8, pp. 3688–3699, 2023.

[83] A. Alhowyan *et al.*, "Antifungal efficacy of itraconazole loaded plga-nanoparticles stabilized by vitamin-e tpgs: In vitro and ex vivo studies," *Journal of Microbiological Methods*, vol. 161, pp. 87–95, 2019.

[84] A. Badawi *et al.*, "Formulation and stability testing of itraconazole crystalline nanoparticles," *AAPS PharmSciTech*, vol. 12, pp. 811–820, 2011.

[85] K. Desai, "Enhanced skin permeation of rofecoxib using topical microemulsion gel," *Drug Development Research*, vol. 63, no. 1, pp. 33–40, 2004.

[86] M. Kumar *et al.*, "Franz diffusion cell and its implication in skin permeation studies," *Journal of Dispersion Science and Technology*, vol. 45, no. 5, pp. 943–956, 2024.

[87] G. Soundarya *et al.*, "Method development and analytical method validation of itraconazole by using uv-visible spectrophotometry," *Indo American Journal of Pharmaceutical Sciences*, vol. 3, no. 5, pp. 487–491, 2016.

[88] OECD, *OECD Guidelines for the Testing of Chemicals*. OECD, 1994.

[89] F. Zothanpuii, R. Rajesh, and K. Selvakumar, "A review on stability testing guidelines of pharmaceutical products," *Asian Journal of Pharmaceutical and Clinical Research*, vol. 13, no. 10, pp. 3–9, 2020.

[90] B. Gajra, C. Dalwadi, and R. Patel, "Formulation and optimization of itraconazole polymeric lipid hybrid nanoparticles (lipomer) using box behnken design," *DARU Journal of Pharmaceutical Sciences*, vol. 23, pp. 1–15, 2015.

[91] K. Wadile, P. Ige, and R. Sonawane, "Preparation of itraconazole nanoparticles and its topical nanogel: Physicochemical properties and stability studies," *International Journal of Pharmaceutical Sciences and Developmental Research*, vol. 5, no. 1, pp. 001–008, 2019.

[92] S. Rana *et al.*, "Design and optimization of itraconazole loaded sln for intranasal administration using central composite design," *Nanoscience & Nanotechnology-Asia*, vol. 10, no. 6, pp. 884–891, 2020.

[93] F. Ullah *et al.*, "Formulation development and characterization of ph responsive polymeric nano-pharmaceuticals for targeted delivery of anti-cancer drug (methotrexate)," *Frontiers in Pharmacology*, vol. 13, p. 911771, 2022.

[94] V. Patravale and P. Desai, "Topical nanointerventions for therapeutic and cosmeceutical applications," in *Focal Controlled Drug Delivery*, pp. 535–560, Springer, 2013.

[95] C. Turan, A. Metin, and Y. Guvenilir, "Controlled release of tetracycline hydrochloride from poly (-pentadecalactone-co--caprolactone)/gelatin nanofibers," *European Journal of Pharmaceutics and Biopharmaceutics*, vol. 162, pp. 59–69, 2021.

[96] E. Altun *et al.*, "Kinetic release studies of antibiotic patches for local transdermal delivery," *Pharmaceutics*, vol. 13, no. 5, p. 613, 2021.

[97] F. Ciftci and A. Özarslan, "Fabrication of polycaprolactone-chitosan/curcumin polymer composite fibers and evaluation of their in vitro release kinetic behaviour and antibacterial-antifungal activity," *Journal of Sol-Gel Science and Technology*, vol. 109, no. 1, pp. 192–203, 2024.

[98] F. Nasr *et al.*, "Preparation and evaluation of contact lenses embedded with polycaprolactone-based nanoparticles for ocular drug delivery," *Biomacromolecules*, vol. 17, no. 2, pp. 485–495, 2016.

[99] W. Badri *et al.*, "Effect of process and formulation parameters on polycaprolactone nanoparticles prepared by solvent displacement," *Colloids and Surfaces A: Physicochemical and Engineering Aspects*, vol. 516, pp. 238–244, 2017.

[100] Z. Zhang *et al.*, "Polymeric nanoparticles-based topical delivery systems for the treatment of dermatological diseases," *Wiley Interdisciplinary Reviews: Nanomedicine and Nanobiotechnology*, vol. 5, no. 3, pp. 205–218, 2013.

[101] M. Danaei *et al.*, "Impact of particle size and polydispersity index on the clinical applications of lipidic nanocarrier systems," *Pharmaceutics*, vol. 10, no. 2, p. 57, 2018.

[102] S. Honary and F. Zahir, "Effect of zeta potential on the properties of nano-drug delivery systems—a review (part 2)," *Tropical Journal of Pharmaceutical Research*, vol. 12, no. 2, pp. 265–273, 2013.

[103] Y. Wan, Z. Gan, and Z. Li, "Effects of the surface charge on the stability of peg-b-pcl micelles: simulation of the interactions between charged micelles and plasma components," *Polymer Chemistry*, vol. 5, no. 5, pp. 1720–1727, 2014.

[104] S. Kumar, "Formulation and characterization of noscapine-loaded polycaprolactone nanoparticles," *Asian Journal of Pharmaceutics (AJP)*, vol. 13, no. 1, 2019.

[105] V. Lemaire, J. Belair, and P. Hildgen, "Structural modeling of drug release from biodegradable porous matrices based on a combined diffusion/erosion process," *International Journal of Pharmaceutics*, vol. 258, no. 1-2, pp. 95–107, 2003.

[106] S. Javaid *et al.*, "Cefotaxime loaded polycaprolactone based polymeric nanoparticles with antifouling properties for in-vitro drug release applications," *Polymers*, vol. 13, no. 13, p. 2180, 2021.

[107] J. Kujawski *et al.*, "Structural and spectroscopic properties of itraconazole and ketoconazole–experimental and theoretical studies," *Journal of Molecular Structure*, vol. 1146, pp. 259–266, 2017.

[108] T. Elzein *et al.*, "Ftir study of polycaprolactone chain organization at interfaces," *Journal of Colloid and Interface Science*, vol. 273, no. 2, pp. 381–387, 2004.

[109] V. Vyas *et al.*, "Physicochemical characterization of solid dispersion systems of tadalafil with poloxamer 407," *Acta Pharmaceutica*, vol. 59, no. 4, pp. 453–461, 2009.

[110] N. Fathima *et al.*, "Drug-excipient interaction and its importance in dosage form development," *Journal of Applied Pharmaceutical Science*, no. Issue, pp. 66–71, 2011.

[111] P. Lucena *et al.*, "In vivo vaginal fungal load reduction after treatment with itraconazole-loaded polycaprolactone-nanoparticles," *Journal of Biomedical Nanotechnology*, vol. 14, no. 7, pp. 1347–1358, 2018.

[112] A. Badawi *et al.*, "Formulation and stability testing of itraconazole crystalline nanoparticles," *AAPS PharmSciTech*, vol. 12, no. 3, pp. 811–820, 2011.

[113] X. Ling *et al.*, "Development of an itraconazole encapsulated polymeric nanoparticle platform for effective antifungal therapy," *Journal of Materials Chemistry B*, vol. 4, no. 10, pp. 1787–1796, 2016.

[114] T. Tao *et al.*, "Preparation and evaluation of itraconazole dihydrochloride for the solubility and dissolution rate enhancement," *International Journal of Pharmaceutics*, vol. 367, no. 1-2, pp. 109–114, 2009.

[115] T. Plivelic *et al.*, "Structure and morphology of poly (-caprolactone)/chlorinated polyethylene (pcl/pecl) blends investigated by dsc, simultaneous saxs/waxd, and elemental mapping by esi-tem," *Macromolecules*, vol. 40, no. 2, pp. 253–265, 2007.

[116] S. Zhang, T. Lee, and A. Chow, "Crystallization of itraconazole polymorphs from melt," *Crystal Growth & Design*, vol. 16, no. 7, pp. 3791–3801, 2016.

[117] F. Veras *et al.*, "Natamycin-loaded electrospun poly (-caprolactone) nanofibers as an innovative platform for antifungal applications," *SN Applied Sciences*, vol. 2, pp. 1–14, 2020.

[118] S. Shin, J. Kim, and I. Oh, "Mucoadhesive and physicochemical characterization of carbopol-poloxamer gels containing triamcinolone acetonide," *Drug Development and Industrial Pharmacy*, vol. 26, no. 3, pp. 307–312, 2000.

[119] P. Bala *et al.*, "Transdermal drug delivery system (tdds)—a multifaceted approach for drug delivery," *Journal of Pharmaceutical Research*, vol. 8, no. 12, pp. 1805–1835, 2014.

[120] A. Waheed *et al.*, "Nanovesicles for the treatment of skin disorders," in *Applications of Nanovesicular Drug Delivery*, pp. 285–302, Elsevier, 2022.

[121] D. Lunter *et al.*, "Progress in topical and transdermal drug delivery research—focus on nanoformulations," *Pharmaceutics*, vol. 16, no. 6, p. 817, 2024.

[122] C. Charmeau-Genevois *et al.*, "A simplified index to quantify the irritation/corrosion potential of chemicals–part i: Skin," *Regulatory Toxicology and Pharmacology*, vol. 123, p. 104922, 2021.

[123] C. Charmeau-Genevois *et al.*, "A simplified index to quantify the irritation/corrosion potential of chemicals–part ii: Eye," *Regulatory Toxicology and Pharmacology*, vol. 123, p. 104935, 2021.

[124] T. Nakamura *et al.*, "Eucalyptus oil reduces allergic reactions and suppresses mast cell degranulation by downregulating ige-fcri signalling," *Scientific Reports*, vol. 10, no. 1, p. 20940, 2020.

[125] S. Tayel *et al.*, "Positively charged polymeric nanoparticle reservoirs of terbinafine hydrochloride: preclinical implications for controlled drug delivery in the aqueous humor of rabbits," *AAPS PharmSciTech*, vol. 14, pp. 782–793, 2013.

[126] M. Sakhi *et al.*, "Effect of polymeric stabilizers on the size and stability of plga paclitaxel nanoparticles," *Saudi Pharmaceutical Journal*, vol. 31, no. 9, p. 101697, 2023.